PB85-214336

Development and Evaluation of an Instantaneous Atmospheric Corrosion Rate Monitor

Rockwell International Corp., Thousand Oaks, CA

Prepared for

Environmental Protection Agency
Research Triangle Park, NC

Jun 85

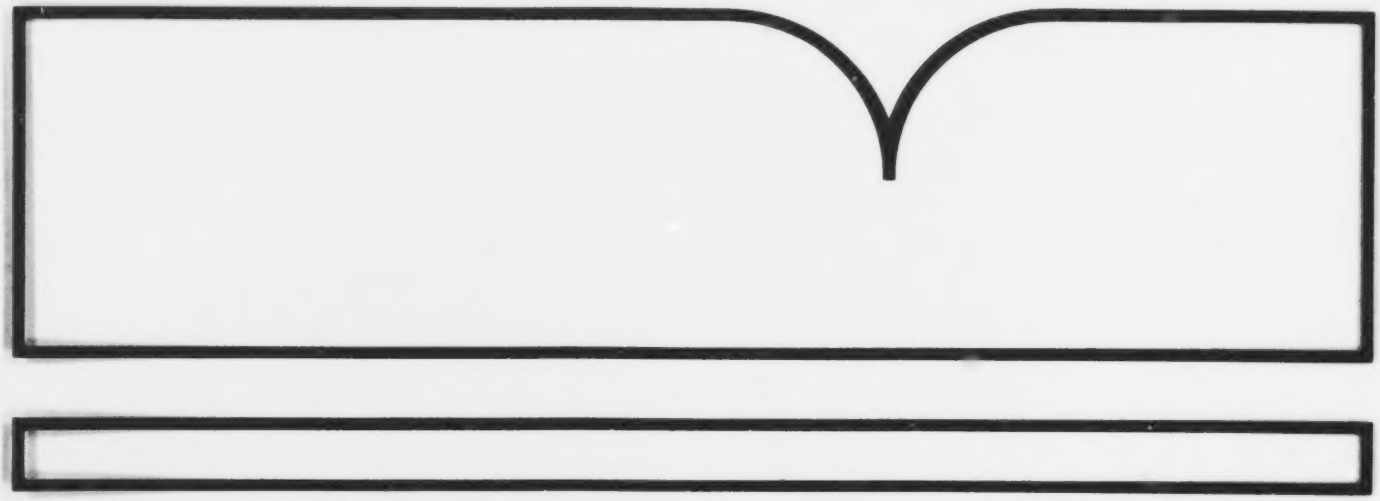

U.S. Department of Commerce
National Technical Information Service
NTIS

PB85-214336

EPA/600/3-85/048
June 1985

DEVELOPMENT AND EVALUATION OF AN INSTANTANEOUS ATMOSPHERIC CORROSION RATE MONITOR

by

F. Mansfeld, S.L. Jeanjaquet and M.W. Kendig
Rockwell International Science Center
Thousand Oaks, CA 91360

and

D.K. Roe
Portland State University
Portland, OR

68-02-3741

Project Officer

Fred H. Haynie
Emissions Measurement and Characterization Division
Atmospheric Sciences and Research Laboratory
Research Triangle Park, NC 27711

ATMOSPHERIC SCIENCES RESEARCH LABORATORY
OFFICE OF RESEARCH AND DEVELOPMENT
U.S. ENVIRONMENTAL PROTECTION AGENCY
RESEARCH TRIANGLE PARK, NC 27711

REPRODUCED BY
NATIONAL TECHNICAL
INFORMATION SERVICE
U.S. DEPARTMENT OF COMMERCE
SPRINGFIELD, VA. 22161

TECHNICAL REPORT DATA
(Please read Instructions on the reverse before completing)

1. REPORT NO. EPA/600/3-85/048	2.
3. RECIPIENT'S ACCESSION NO. PB85 214336/AS	
4. TITLE AND SUBTITLE DEVELOPMENT AND EVALUATION OF AN INSTANTANEOUS ATMOSPHERIC CORROSION RATE MONITOR	5. REPORT DATE June 1985
	6. PERFORMING ORGANIZATION CODE
7. AUTHOR(S) F. Mansfeld, S.K. Jeanjaquet, M.W. Kendig and D.K. Roe	8. PERFORMING ORGANIZATION REPORT NO.
9. PERFORMING ORGANIZATION NAME AND ADDRESS Rockwell International Science Center Thousand Oaks, CA 91360 and Portland State University Portland, OR	10. PROGRAM ELEMENT NO. CDTA1D-06 2067 (FY-85)
	11. CONTRACT/GRANT NO. 68-02-3741
12. SPONSORING AGENCY NAME AND ADDRESS Atmospheric Sciences Research Laboratory - RTP, NC Office of Research and Development U.S. Environmental Protection Agency Research Triangle Park, N.C. 27711	13. TYPE OF REPORT AND PERIOD COVERED Final
	14. SPONSORING AGENCY CODE EPA/600/09
15. SUPPLEMENTARY NOTES	

16. ABSTRACT

A research program has been carried out in which a new instantaneous atmospheric corrosion rate monitor (ACRM) has been developed and evaluated, and equipment has been constructed which will allow the use of many sensors in an economical way in outdoor exposures. In the first task, the ACRM was developed and tested in flow chambers in which relative humidity and gaseous and particulate pollutant levels can be controlled. Diurnal cycles and periods of rain have been simulated. The effects of aerosols have been studied. A computerized system was used for collection, storage, and analysis of the electrochemical data. In the second task, a relatively inexpensive electronics system for control of the ACRM and measurement of atmospheric corrosion rates which was designed and built under a subcontract at Portland State University was tested. In the third task, calibration of deterioration rates of various metallic and nonmetallic materials with the response of the ACRMs attached to these materials was carried out under controlled environmental conditions using the system developed in the second task. A Quality Assurance project plan has been prepared with inputs from the Rockwell International Environmental Monitoring and Service Center and Quality Assurance System audits have been performed.

17. KEY WORDS AND DOCUMENT ANALYSIS

a. DESCRIPTORS	b. IDENTIFIERS/OPEN ENDED TERMS	c. COSATI Field/Group

18. DISTRIBUTION STATEMENT RELEASE TO PUBLIC	19. SECURITY CLASS *(This Report)* UNCLASSIFIED	21. NO. OF PAGES 84
	20. SECURITY CLASS *(This page)* UNCLASSIFIED	22. PRICE

EPA Form 2220-1 (Rev. 4-77) PREVIOUS EDITION IS OBSOLETE

The information in this document has been funded by the United States Environmental Protection Agency under contract 68-02-3741 to Rockwell International Science Center. It has been subjected to Agency review and approval for publication.

Mention of trade names or commercial products does not constitute endorsement or recommendation for use.

ABSTRACT

A research program has been carried out in which a new instantaneous atmospheric corrosion rate monitor (ACRM) has been developed and evaluated, and equipment has been constructed which will allow the use of many sensors in an economical way in outdoor exposures. The research program consisted of three tasks. In the first task, the ACRM was developed and tested in flow chambers in which relative humidity and gaseous and particulate pollutant levels can be controlled. Diurnal cycles and periods of rain have been simulated. The effects of aerosols have been studied. A computerized system was used for collection, storage, and analysis of the electrochemical data. In the second task a relatively inexpensive electronics system for control of the ACRM and measurement of atmospheric corrosion rates which was designed and built under a subcontract at Portland State University was tested. In the third task, a calibration of deterioration rates of various metallic and nonmetallic materials with the response of the ACRMs attached to these materials was carried out under controlled environmental conditions using the system developed in the second task. A Ouality Assurance project plan has been prepared with inputs from the Rockwell International Environmental Monitoring and Service Center and Quality Assurance System audits have been performed.

CONTENTS

ABSTRACT..... iii
FIGURES..... vi
TABLES..... vii
1.0 INTRODUCTION..... 1
2.0 THE NEW ATMOSPHERIC CORROSION RATE MONITOR (ACRM)..... 4
2.1 Design of the ACRM and Measurement Principle..... 4
3.0 RESPONSE TO VARIATIONS IN ENVIRONMENTAL CONDITIONS (TASK I)..... 8
3.1 Effect of Pretreatment and Exposure to Single Pollutants on ACRM Response..... 8
3.2 Effect of Exposure to Combination of Pollutants and UV Light..... 16
3.3 Effect of Exposure to Pollutants, Simulated Rain Cycles and UV Light..... 20
3.4 Effect of Exposure of Pollutants and Aerosols..... 24
4.0 DESIGN AND TEST OF THE DATA LOGGING SYSTEM (ACRMDL) (TASK II)..... 29
5.0 CORRELATION OF SENSOR RESPONSE WITH DETERIORATION OF DIFFERENT MATERIALS (TASK III)..... 36
6.0 SUMMARY AND CONCLUSIONS..... 48
7.0 REFERENCES..... 50
APPENDIX I..... 52
PROCEDURE FOR PERFORMING ATMOSPHERIC CORROSION RATE MEASUREMENTS.... 52
APPENDIX II..... 59
ATMOSPHERIC CORROSION RATE METER AND DATA LOGGER (ACRMDL)..... 59

FIGURES

Number		Page
1	Design of ACRM and electronic circuit	5
2	Photograph of sensor part of ACRM after corrosion test	6
3	Block diagram of measurement system	7
4	Experimental arrangement for ACRM tests under controlled conditions. The ACRMDL is used to run the electrochemical tests	9
5	Test cell, gas mixing system and ACRMDL	10
6	Sensor arrangement in test cell	11
7	Response of eight ACRMs to RH after pretreatment with 1 mM $CaCl_2$	12
8	Effect of pollutant nature and concentration on ACRM response ($CaCl_2$ pretreatment) (a) SO_2, (b) NO_2, (c) O_3	14
9	Response of sensor No. 1 to four different combinations of pollutants and UV light	17
10	Response of sensor No. 4 to four different combinations of pollutants and UV light	18
11	Response of sensor No. 8 to four different combinations of pollutants and UV light	18
12	Pollutant concentration and polarization resistance R_p as a function of time and environment conditions for four sensors exposed on three successive days	23
13	Polarization resistance R_p during exposure to H_2SO_4 aerosol (Fig. 13a) and acetic acid aerosol (Fig. 13b) with and without presence of pollutants	25
14	Photograph of two sensors after exposure to acetic acid aerosol	27

FIGURES (Continued)

Number		Page
15	Plot of ACRM data for three sensors as recorded with the ACRMDL	30
16	Sensor response for changes in environmental conditions for four cycles. Sensor No. 2 has H_2O pretreatment, sensor No. 5 is without pretreatment	32
17	Response of four ACRMs with different pretreatments to changes in environmental conditions	34
18	Environmental changes and response of an ACRM	37
19	Two 80 h test cycles for six ACRMs	38
20	Schematic of ACRM and test coupon location	40
21	Time dependence of R_p for six ACRMs during entire test period	42
22	SO_2 concentration at test cell outlet during "wet" and "dry" periods. Also shown are the corresponding maxima and minima values of RH. The drop of the SO_2-concentration is due to a change to a new tank of SO_2	45
23	Integrated corrosion loss of a given time period ("corrosion rate") as a function of exposure time for the six ACRMS	46

TABLES

Number		Page
I	Schedule for First Test Series	13
II	Integrated Corrosion Loss (10^{-3} s/Ω) for Test Series No. 1	16
III	Integrated Corrosion Loss (in 10^{-2} s/Ω) for the Eight Sensors of Test Series No. 2	20
IV	Integrated Corrosion Loss for Test Series No. 3 (s/Ω)	21
V	Corrosion Loss (s/Ω) for Zinc ACRMs	28
VI	Integrated Corrosion Loss (s/Ω) for Six ACRMs During a Four Day Cycle of RH and Pollutants	31
VII	Integrated Corrosion Loss for Exposure to NO_2 (10^{-2} s/Ω)	33
VIII	Integrared Corrosion Loss (s/Ω) for Exposure to SO_2 During Cooling	35
IX	Comparison of Weight Loss and ACRM Data for 31 Day Exposure Test	35

1.0 INTRODUCTION

Since atmospheric corrosion can be assumed to be an electrochemical process, it is quite logical to use electrochemical techniques for monitoring atmospheric corrosion phenomena. These techniques have the important advantages that the atmospheric corrosion behavior can be monitored continuously and that correlations can be established with atmospheric parameters which are recorded at the same location. The development of corrosion sensors for atmospheric corrosion studies has been relatively slow when compared to application of corrosion sensors to other corrosion phenomena. The approach of several groups that have been using electrochemical sensors in atmospheric corrosion research has been reviewed recently (1-4). The main activities have been in Canada by Sereda (5) who developed a concept to monitor the time-of-wetness t_w, in Scandinavia, where Kucera (6) and Haagenrud (7) have applied electrochemical sensors to measurements of t_w and atmospheric corrosion rates, in the USSR, where Mikhailovskii and co-workers are carrying out an extensive program in atmospheric corrosion research (8), and in the United States, where the principal investigator of this project and his co-workers have carried out systematic atmospheric corrosion research using electrochemical techniques. In these studies, the atmospheric corrosion monitor (ACM), which is an electrochemical sensor, has been used to monitor the time-of-wetness (9-15) and atmospheric corrosion rates (12,13) in outdoor exposure (14,15) and laboratory studies (9-13). Most recently, a detailed statistical analysis has been carried out in which the factors that affect the response of ACMs and the reproducibility of ACM data have been determined (2,13). These factors included environmental parameters such as relative humidity (t_w) and SO_2 concentration, heat of the metal used to assemble an ACM, location in the test cell, aging in outdoor exposure, etc.

The new atmospheric corrosion rate monitor (ACRM) which was developed and tested in this program is based on the Sereda's concept (16) which is the basis for ASTM G84 "Standard Practice for Measuring the Time-of-Wetness on Surfaces Exposed to Wetting Conditions as in Atmospheric Corrosion Testing."

The geometry of this sensor promises a much faster response to rapidly changing atmospheric conditions than the more bulky ACMs. While the ASTM document describes only the approach to measure time-of-wetness, the present effort has focused on using the same sensor to determine atmospheric corrosion rates which can be used to determine the corrosivity of test sites, follow corrosion episodes such as acid rain, give an indirect measure of the corrosion behavior of different materials of construction, etc. The new ACRM is a two-electrode system with zinc electrodes which can be attached to the metal of interest. The time-of-wetness t_w would be a by-product of corrosion rate measurements in outdoor exposure, since corrosion activity occurs only during t_w.

Atmospheric corrosion sensors can be designed as galvanic cells such as Cu/Zn, Cu/steel, etc., or as one-metal, two-electrode cells such as steel/steel, Zn/Zn, etc. Both approaches have been used earlier at the Science Center (9-13). In the present program a Zn/Zn sensor was used to which a 30 mV potentiostatic pulse is applied (12,13). In this case, the corrosion current density i_{corr} can, in principle, be calculated from the Stern-Geary equation:

$$i_{corr} = \frac{B}{R_p} = \frac{2b_a \times I_{30}}{2.3\ \Delta E \times A} = k\,\frac{I_{30}}{A} \quad , \quad \text{where} \quad B = \frac{b_a}{2.3}$$

$$\text{and} \quad k = \frac{2b_a}{2.3\Delta E} = \frac{B}{\Delta E} \quad . \qquad (1)$$

Application of Eq. (1) requires the knowledge of the factor B, which depends on the anodic Tafel slope b_a in the case of diffusion control of the cathodic reaction ($b_c \to \infty$). A is the area of one of the two electrodes. For an anodic Tafel slope of b_a = 60 mV and ΔE = 30 mV, k ≃ 1.75. Since the parameter B can change with environmental conditions and with time, and because its exact value often is unknown for a given application, a theoretical value is often used for B (or k) in Eq. (1). Theoretical values of B range from B = 6.5 mV

to 52.1 mV, although B = 13 mV to 26 mV seems to be most common (17). The electrochemical measurement carried out here is, therefore, basically a determination of the polarization resistance R_p.

In order to evaluate the performance of the new ACRM, optimize its response and test the response to variations in the corrosivity of the environment, three tasks have been carried out. In the first task, which formed the basic effort, the ACRM was developed and tested using the laboratory facilities developed previously by Harker (18) and Mansfeld (13) in which wind velocity profiles, temperature, RH, and gaseous and particulate pollutant levels can be controlled. Diurnal cycles and period of rain were simulated. In the second task, a relatively inexpensive electronics system for data logging and control (ACRMDL) of the sensors developed in the first task and for measurement of atmospheric corrosion rates was developed and tested. In the third task it was determined whether the corrosion sensor response can be used as a proxy for the atmospheric corrosion behavior of a variety of materials such as galvanized steel, weathering steel, marble, and latex or oil base house paints.

2.0 THE NEW ATMOSPHERIC CORROSION RATE MONITOR (ACRM)

The design of the new miniature atmospheric corrosion rate monitor (ACRM) is based on the sensor used by Sereda (16) which is now the basis of ASTM G84. The advantage is its small size which makes it possible to attach it to a material of interest and monitor the time-of-wetness t_w for this material in its microclimate and determine a (indirect) measure of the instantaneous corrosion rate of this material. Since the sensor output only reflects the corrosion rate of the sensor material, in this case zinc, conversion factors have to be established to calculate corrosion rates for other materials. This question has been addressed in Task III. An alternative approach would be to calculate a corrosivity index for a given microclimate based on the ACRM corrosion rate data.

2.1 Design of the ACRM and Measurement Principle

The design of the ACRM is shown schematically in Fig. 1. A photograph of the sensor part taken after a corrosion test is shown in Fig. 2. An important improvement over Sereda's original design (16) is the use of solid zinc instead of zinc-plated copper which avoids the problem of porosity of the zinc layer after extended exposure periods and accelerated corrosion due to the Zn/Cu couple which would also cause errors in the measurement. The measurement principle is, of course, drastically different since Sereda et al (16) used a galvanic couple Zn/Au or Cu/Au to measure t_w, whereas in the present project the polarization resistance technique (17) is used to measure instantaneous corrosion rates.

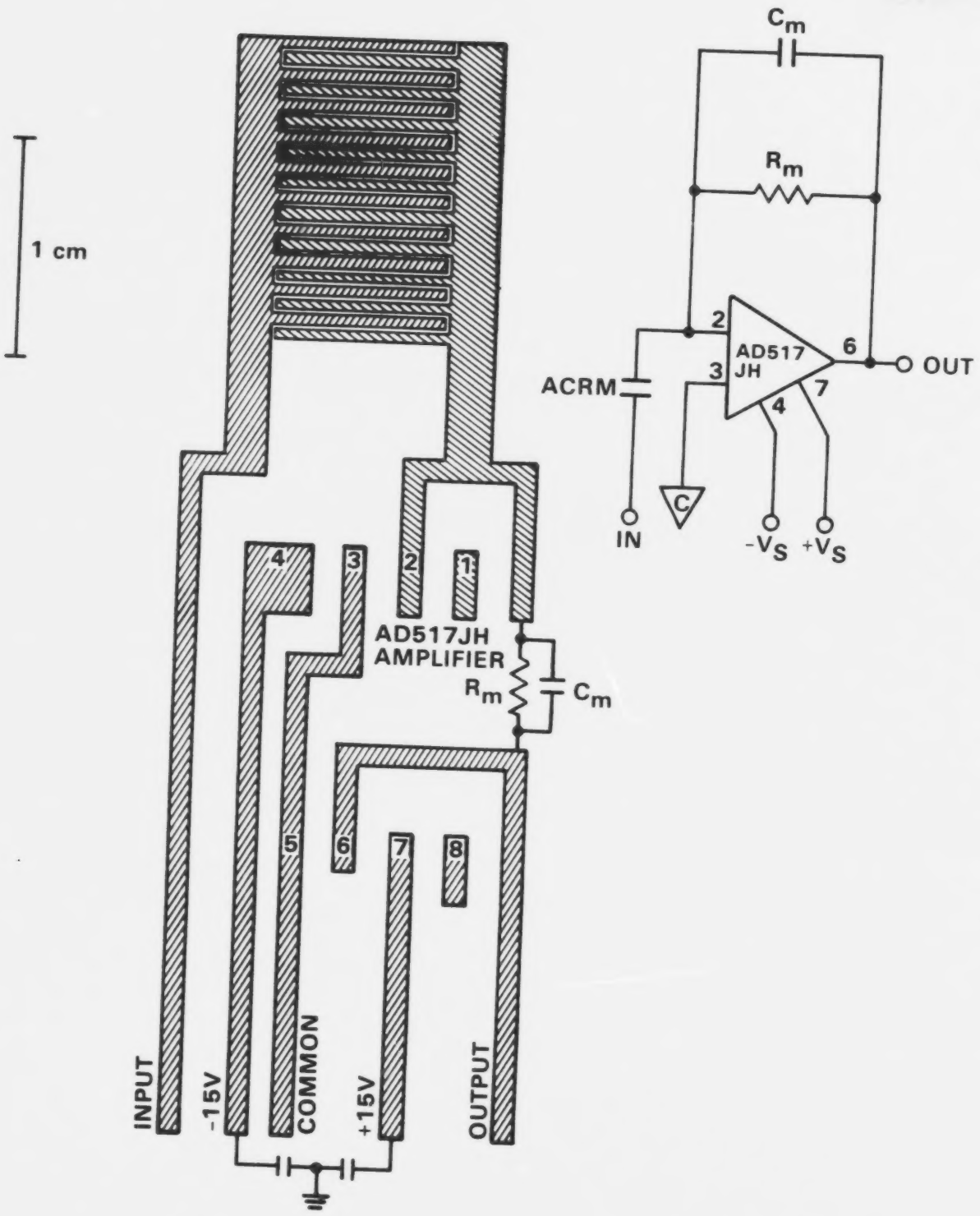

Fig. 1 Design of ACRM and electronic circuit.

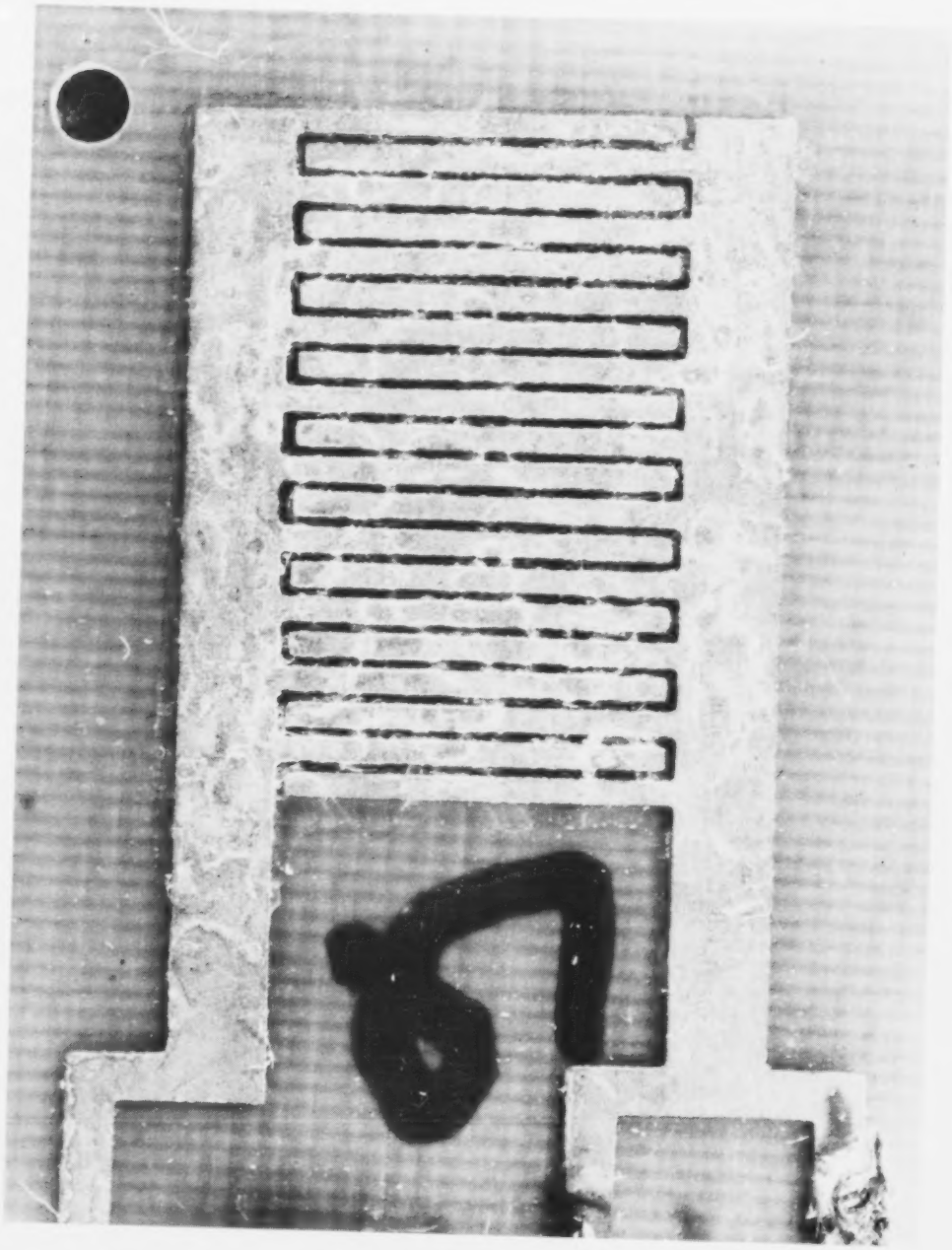

Fig. 2 Photograph of sensor part of ACRM after corrosion test.

The use of solid zinc initially posed certain problems in producing sensors with the exact dimensions shown in Fig. 1. Electronic Controls Designs developed an etching technique to produce sensors of the desired tolerances. The thickness of the zinc sensors used in this project is 0.05 mm; it is bonded to an epoxy laminate board of 0.25 mm. The sensor "fingers" are 7.8 mm long, 0.6 mm wide and are spaced 0.2 mm apart (Figs. 1 and 2). The active part of the sensor measures 19 mm × 12.3 mm, the remainder is used for connection of the current amplifier, capacitors and leads which connect the sensor to the control unit.

Figure 1 also shows the electronic circuit for measurement of the current flow as a result of application of a ± 30 mV pulse. This potential pulse is produced by the D/A card in the multiprogrammer of the computerized system which controls the experiment. A schematic is shown in Fig. 3. The potential pulse is applied between the INPUT and COMMON terminals of the sensor as shown in Fig. 1. The current I is determined from the output V of the amplifier as $I = V/R_m$, where R_m is the measuring resistor. A more detailed description of the measurement principle is given in Appendix I, which also give details concerning the control of the environmental parameters. The test series in Task III was conducted with the measurement system developed in Task II by Prof. D.K. Roe of Portland State University.

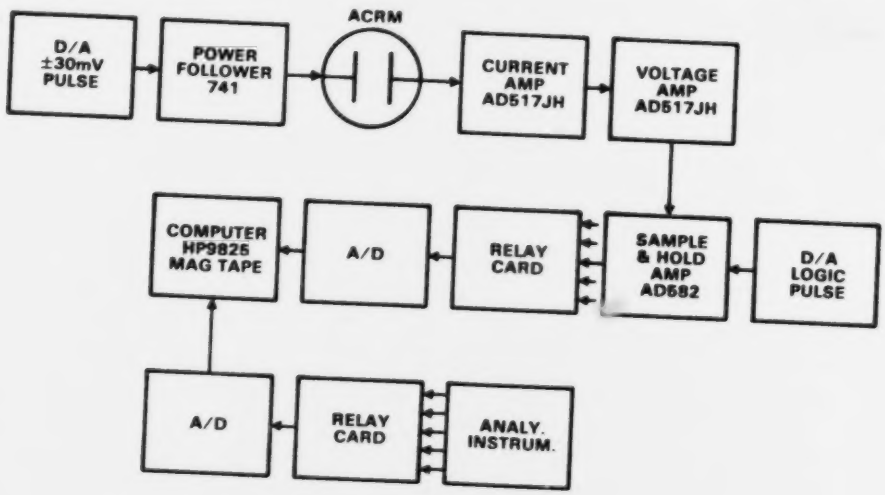

Fig. 3 Block diagram of measurement system.

3.0 RESPONSE TO VARIATIONS IN ENVIRONMENTAL CONDITIONS (TASK I)

The response of the ACRM to various environments and environmental changes was evaluated by exposing ACRMs to controlled atmospheres containing different single pollutants or their combinations, simulated diurnal cycles and two different aerosols. The experimental arrangement for this task, which was also used in Task II and III for control of environmental conditions, is shown in Figs. 4-6. Details are given in Appendix I. Figure 4 shows the test cell with a quartz cover which contains the sensors, the gas mixing apparatus, the SO_2 and NO_2 analyzers and the RH meter. Figure 4 was taken during Task II when the computer-controlled system for the electrochemical measurements was replaced by the ACRM data logger (ACRMDL). Figure 5 shows in more detail the test cell, the mixing system for dry and wet air for adjustment of the RH, the flowmeter for controlling the pollutant concentrations, and the ACRMDL. The feed-through for the connections between the sensors and the ACRMDL can be seen. A close-up of six sensors attached to the bottom of test cell and the connections are shown in Fig. 6. Since the ACRMDL was used when the picture was taken, the amplifiers used in the early measurements (Fig. 1) are not used.

3.1 Effect of Pretreatment and Exposure to Single Pollutants on ACRM Response

Research at this laboratory and by others has shown (4) that the chemical nature of the corrosion product layer has a great influence on the critical RH-level at which condensation occurs. The time-of-wetness is therefore strongly affected by the chemistry of the corrosion product layer and one can assume that the corrosion rate and its changes with time depend also on this chemistry. It was therefore necessary to evaluate the effects of different pretreatments on sensor response and stability.

The sensors were pretreated with 1 mM NaCl, $CaCl_2$, deionized water or were untreated (see also Appendix I). They were then exposed to a RH-cycle of 65%-80%-95%-80%-65% for one hour each.

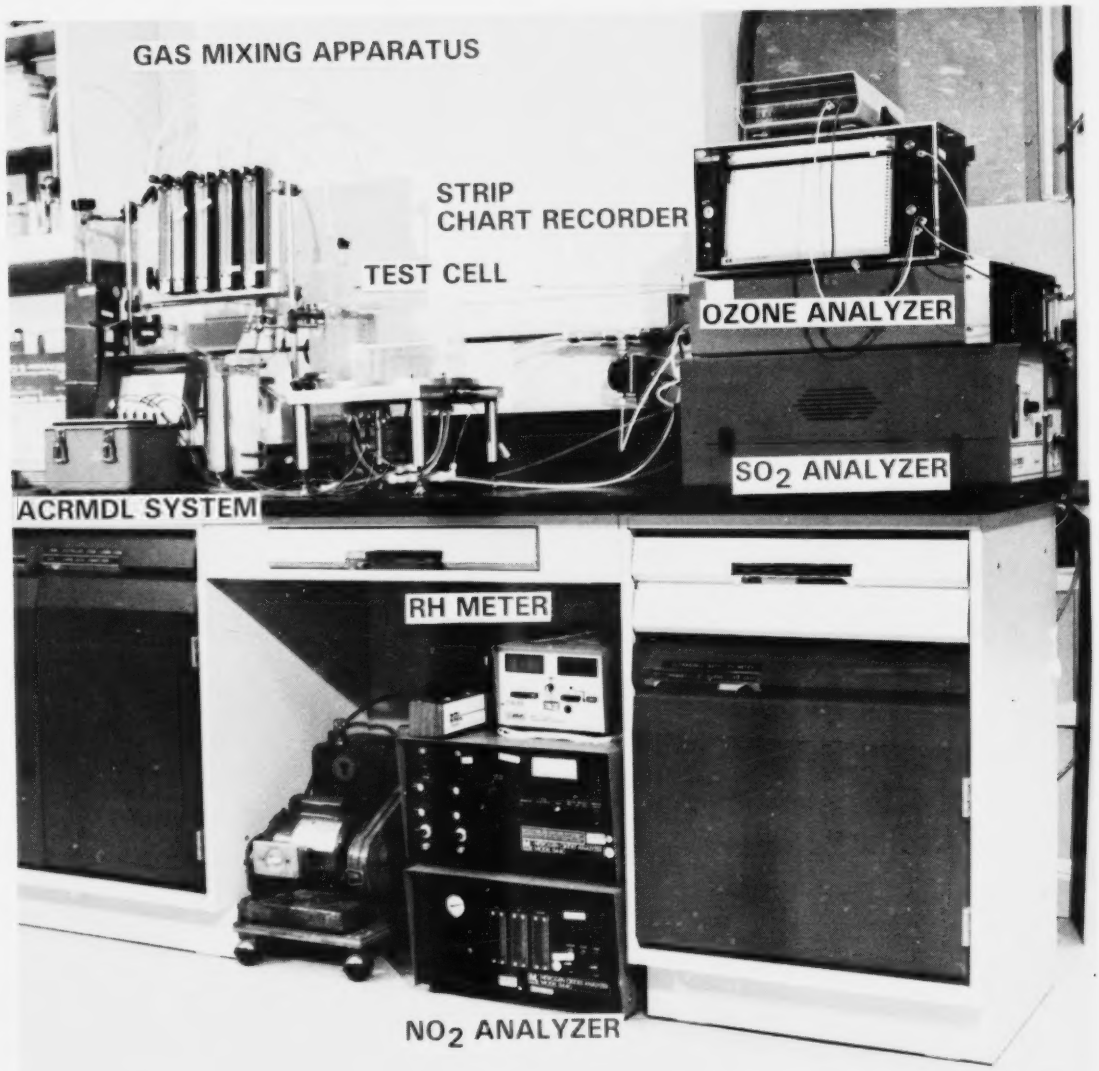

Fig. 4 Experimental arrangement for ACRM tests under controlled conditions. The ACRMDL is used to run the electrochemical tests.

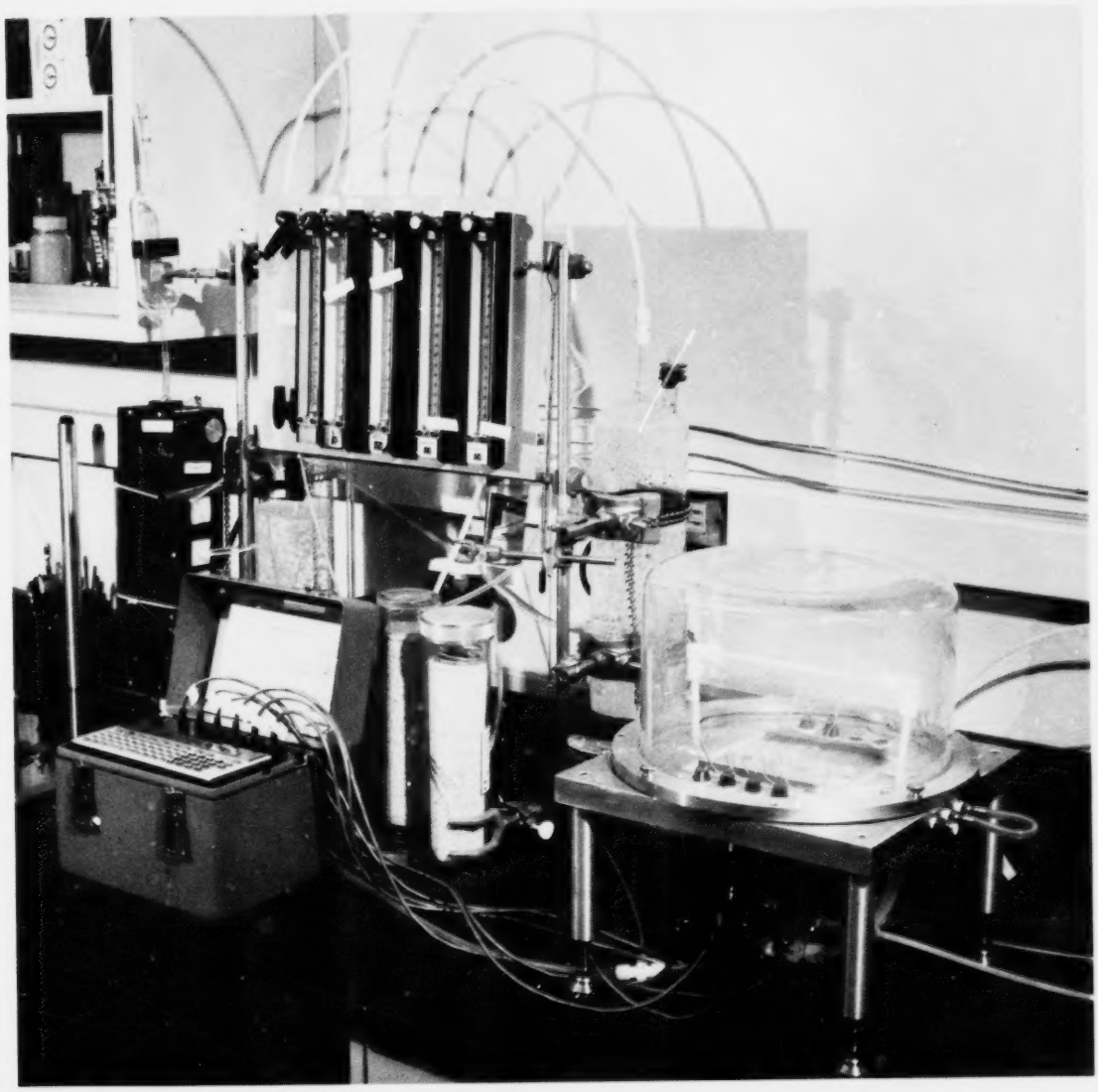

Fig. 5 Test cell, gas mixing system and ACRMDL.

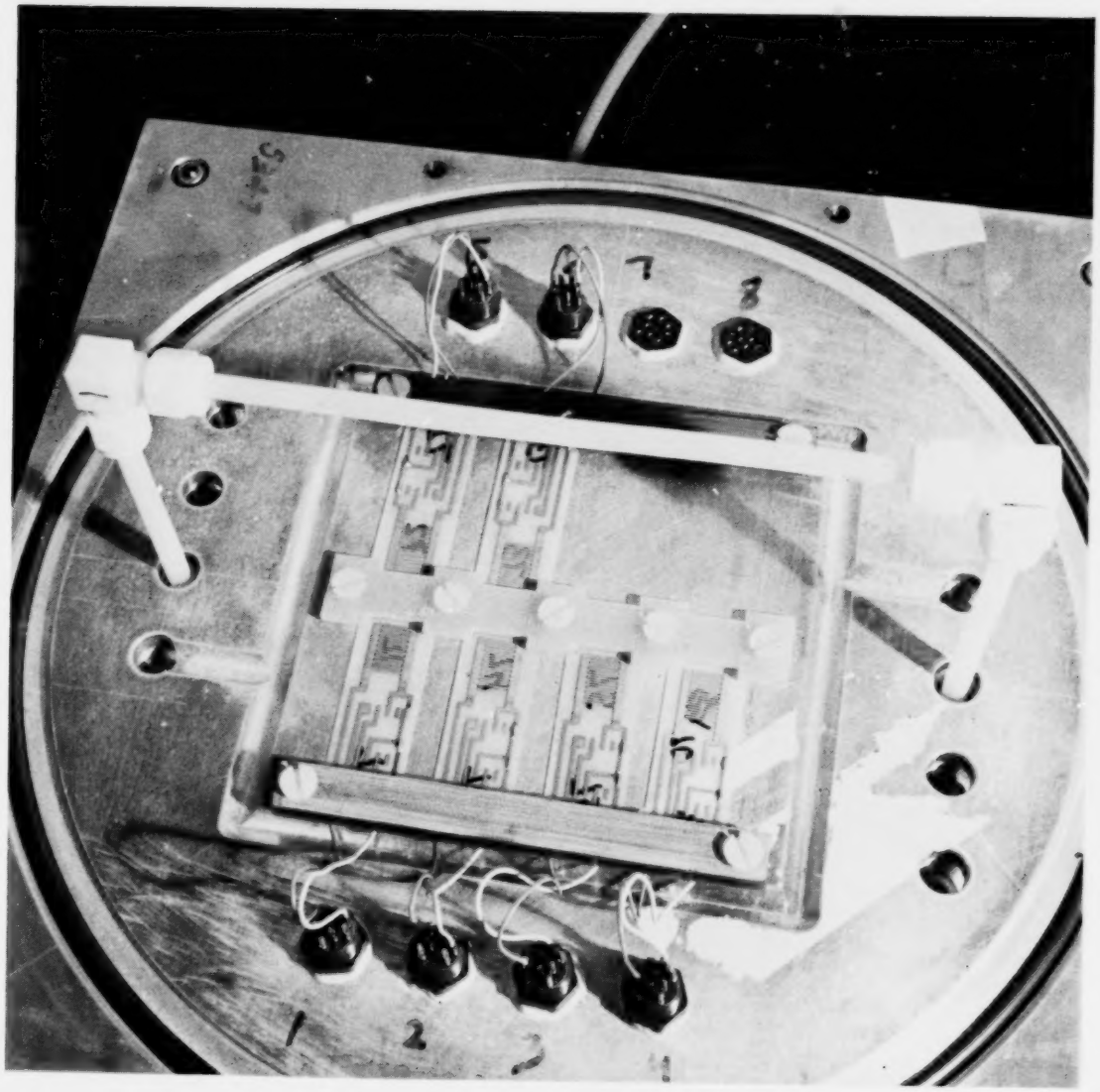

Fig. 6 Sensor arrangement in test cell.

Figure 7 shows the response of eight ACRMs to RH after pretreatment with $CaCl_2$. A pronounced effect of RH is seen with fairly similar response of the sensors except for No. 3 which in the early stages of the experiment showed higher current flow. The R_p-values are fairly large since only a very small current flows during exposure of a dry surface to RH in the absence of pollutants; similar results were observed for the NaCl pretreatment. For H_2O pretreatment and without a pretreatment, the current flow was very low and often below the detection limit of the system. This set of data was taken, therefore, more as a qualitative indication of the necessity of an effective, reproducible pretreatment.

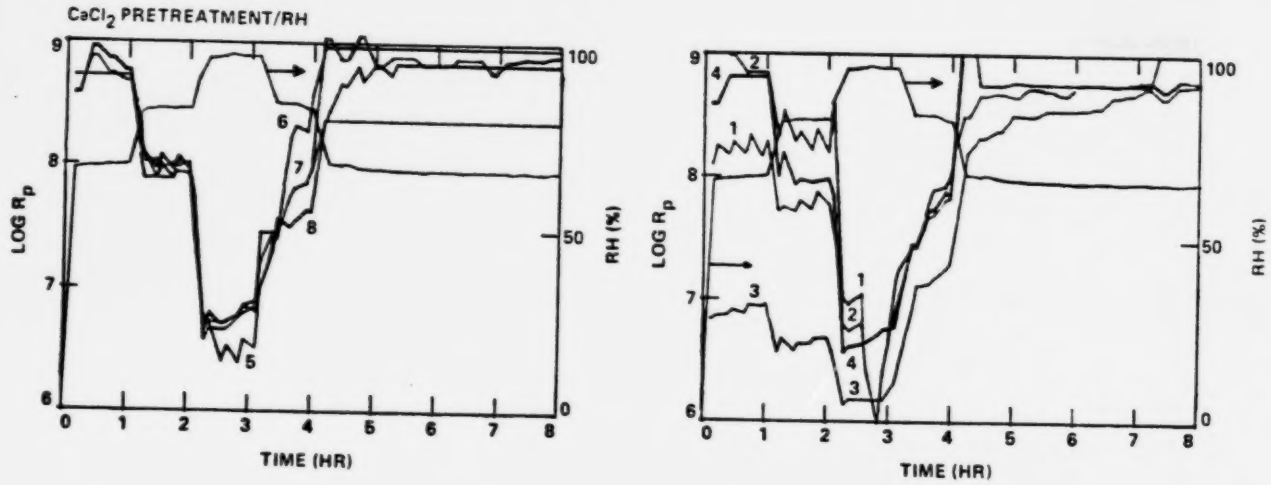

Fig. 7 Response of eight ACRMs to RH after pretreatment with 1 mM $CaCl_2$.

Table I explains the test sequence for the first test series in which the effect of sensor pretreatment and nature of pollutant was evaluated. For each subset of this series, eight ACRMs were pretreated according to the four possibilities Ia-d and then subjected to the sequence under II in Table I. Two

Table I

Schedule for First Test Series

I. Effect of Pretreatment
a. dist. H_2O b. NaCl (1 mM) c. $CaCl_2$ (1 mM) d. None Cycle RH = 65-80-95% and back, 1 h each
II. Effect of Pollutants
1. Sensors No. 1, 2 with pretreatment a, + CPM Sensors No. 3, 4 with pretreatment a, RH = 90%, 2 h 2. $[SO_2]$ = hi → low → stepwise to hi, 1 h each 3. RH = 90% for 1 h, followed by RH = 65% overnight 4. Add sensors No. 5, 6, RH = 90% for 1 h 5. Repeat 2. and 3. for NO_2 6. Add sensors No. 7, 8, RH = 90% for 1 h 7. Repeat 2. and 3. for O_3 Same for pretreatments b,-d (sensors No. 9-32) Add zinc pieces (2 each) for weight loss, in steps 1, 4 and 6 Particulate matter is applied only in Step 1

sensors (e.g., Nos. 1 and 2) were coated with carbonaceous particulate matter (CPM) as explained in Appendix I to an extent which was equivalent to 0.5 years exposure in an urban environment. These two sensors and two additional (e.g., Nos. 3 and 4) were then exposed for 2 h at RH = 90% and R_p-values were determined continuously. As shown in Fig. 8a the SO_2 level was increased to 1 ppm for 1 h and then changed stepwise to 0.1, 0.5 and 1.0 ppm for 1 h each. The SO_2 was then turned off and after another hour at RH = 90%, the RH was reduced to 65% overnight. Figure 8a shows the response of these four ACRMs from steps II.1 to II.3 in Table 1. The next morning two additional sensors (e.g., Nos. 5 and 6) were added to the test cell and the cycle repeated for NO_2 (steps II.4 and II.5) (see Fig. 8b). On the last day the pollutant was O_3. Zinc coupons were added with each set of sensors (Fig. 8c).

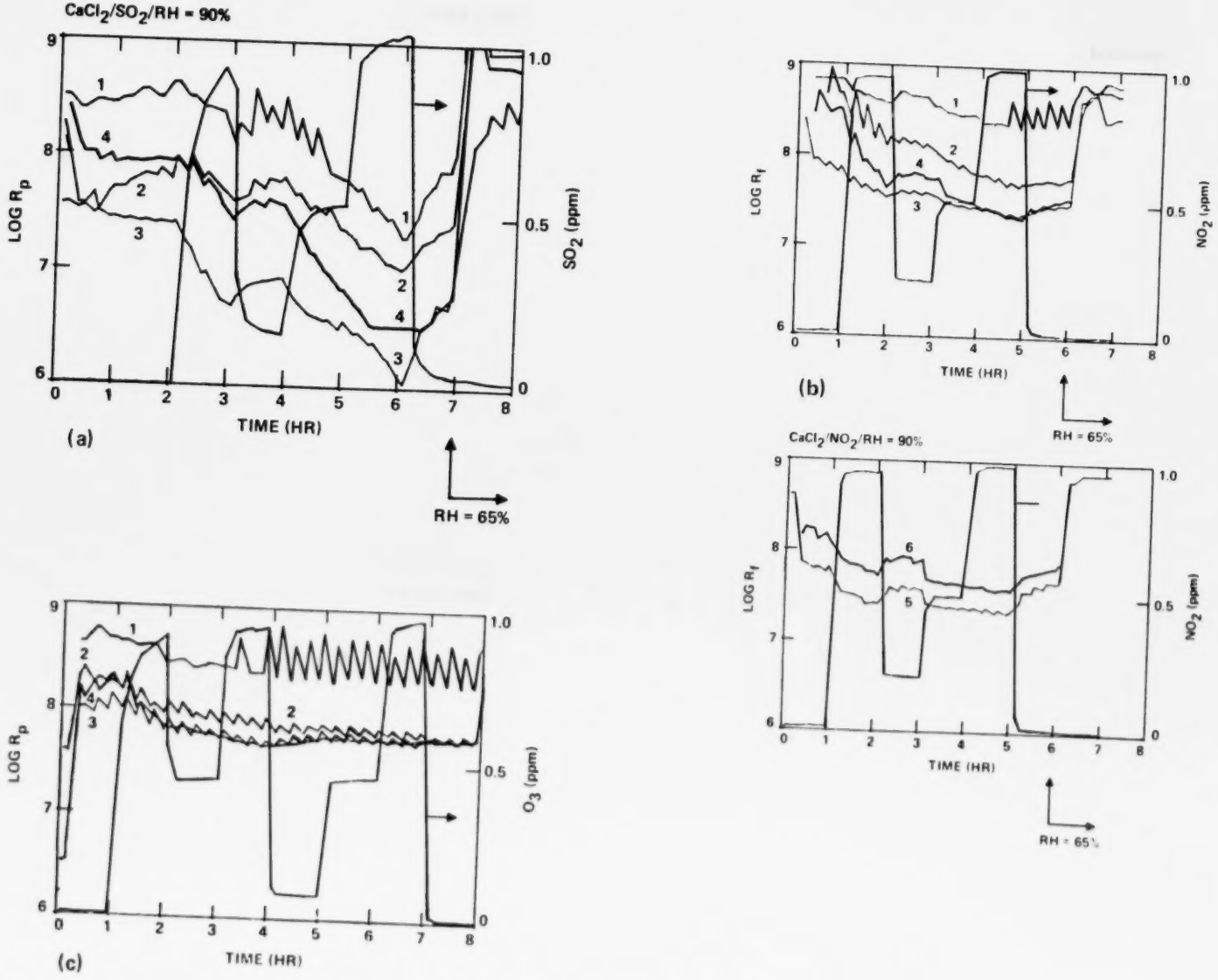

Fig. 8 Effect of pollutant nature and concentration on ACRM response ($CaCl_2$ pretreatment). (a) SO_2. (b) NO_2. (c) O_3.

As a result of this particular test sequence (Table I), sensors Nos. 1-4 and the corresponding zinc coupons were exposed to $SO_2 + NO_2 + O_3$, sensors Nos. 5 and 6 to NO_2 and O_3, while sensors Nos. 7 and 8 experience only exposure to O_3. A comparison of the corrosion behavior of sensors Nos. 1 and 2 with sensors Nos. 3 and 4 should allow an estimate of the effect of CPM on the corrosion behavior.

SO_2 has a strong effect on the corrosion rate of the zinc sensor as can be seen in Fig. 8a where the polarization resistance decreased almost immediately when the SO_2 level was increased to 1 ppm. This effect is not due to increased conductivity of the surface electrolyte (as could be argued) as can be seen from the almost instantaneous increase of R_p when the SO_2 level is decreased to 0.1 ppm. There is no clear distinction between sensors Nos. 1 and 2 which are coated with CPM and sensors Nos. 3 and 4. NO_2 also affect corrosion rates as can be seen from the changes of R_p following the changes of the NO_2 level. O_3, on the other hand, seems to have a passivating effect and no clear changes of R_p with ozone level can be detected. Similar behavior was observed for the NaCl pretreatment. For the H_2O pretreatment the current flow was very low and often under the detection limit of the system. It has to be considered that for $R_p = 10^9$ ohm, the current I equals $\Delta E/R_p = 30\ mV \cdot 10^{-9}$ ohm = 30 nA. At such low current levels, electrical noise problems affect the accuracy of the measurement severely.

Integration of the R_p^{-1}-time curves for the time when pollutants were present gives the corrosion loss (in ohms/s) shown in Table II. Since the parameter B (Eq. (1)) is not known for the present experimental conditions, it is preferable to use as a qualitative measure of the corrosion effects, the integrated corrosion loss as shown in Table II. Coating with CPM lowers the corrosion loss for $CaCl_2$ and for NaCl pretreatments (Table II). Sensors Nos. 1 and 3 are compared with Nos. 3 and 4. A comparison of Sensors Nos. 7 and 8 with Nos. 5 and 6 and with Nos. 3 and 4 shows that exposure to SO_2 produces a larger corrosion loss than exposure to NO_2, while O_3 exposure induces the lowest corrosion damage. Pretreatment with NaCl leads to higher corrosion rates than $CaCl_2$. A comparison of sensors Nos. 3 and 4 with Nos. 5 and 6 shows no large effect of prior exposure to SO_2 (Sensors Nos. 3 and 4) on

Table II

Integrated Corrosion Loss (10^{-3} s/Ω) for Test Series No. 1

PT	Pollutant	ACRM No. 1	2	3	4	5	6	7	8
$CaCl_2$	SO_2	0.27	0.81	4.89	2.32				
$CaCl_2$	NO_2	0.06	0.24	0.63	0.60	0.67	0.38		
$CaCl_2$	O_3	0.10	0.37	0.45	0.63	0.20	0.18	0.08	0.09
Total		0.43	1.42	5.97	3.55	0.87	0.57	0.08	0.09
NaCl	SO_2	0.30	0.72	7.36	6.59				
NaCl	NO_2	0.55	0.69	3.08	4.59	3.90	3.34		
NaCl	O_3	0.40	0.50	2.56	2.43	2.47	2.27	2.58	3.38
Total		1.25	1.91	13.00	13.61	6.37	5.61	2.58	3.38

corrosion losses during exposure to NO_2. Similarly, Sensors Nos. 3-8 show very similar corrosion losses during exposure to O_3 especially for the NaCl pretreatment. This lack of an effect of prior exposure to a different pollutant is somewhat surprising, since it would be expected that the resulting changes of surface chemistry also change t_w and corrosion rates. However, the short exposure periods which had to be used in the present tests might have precluded significant changes of surface chemistry.

3.2 Effect of Exposure to Combination of Pollutants and UV Light

In the second series of experiments the ACRMs were exposed to SO_2 + NO_2, SO_2 + O_3, O_3 + NO_2 and SO_2 + NO_2 + O_3 at 1 ppm for each pollutant. A UV lamp was turned on and off every hour during the 4 h exposure to each combination of pollutants.

In this second series two sensors (Nos. 1, 2) from the first series were used which were pretreated with $CaCl_2$ and CPM and had been tested in the first series. In addition, six new sensors were used which were all pretreated

three (Nos. 6-8) were coated with CPM. All eight sensors were first exposed to the RH-cycle as before. It was noted that the current flow at each RH was less than in the first series which could be due to the fact that the sensors were stored in a desiccator over the weekend before the RH-test.

In the main experiment the sensors were first exposed to RH = 90% for 2 h. After that a combination of two pollutants (or all three at the fourth day) was introduced at a level of 1 ppm for each. After 1 h a UV lamp was turned on for 1 h as shown in Figs. 9-11. After a total test time of 6 h, the light and the pollutants were turned off and after another hour RH was reduced to 65%.

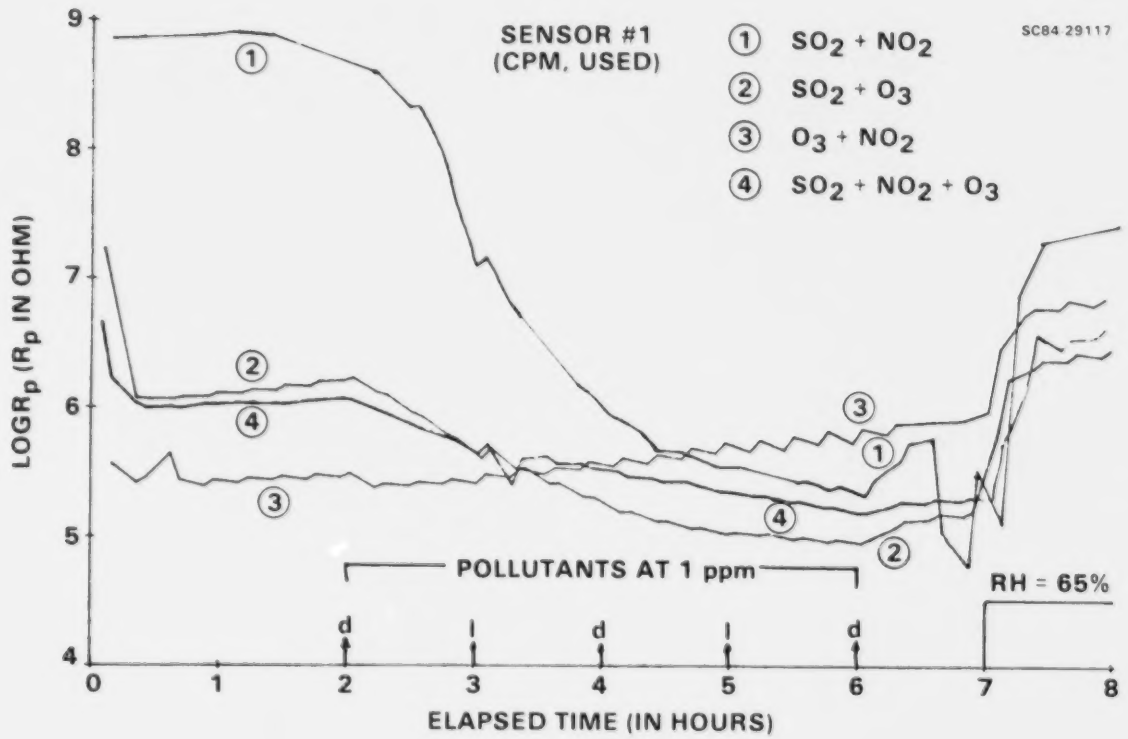

Fig. 9 Response of Sensor No. 1 to four different combinations of pollutants and UV light.

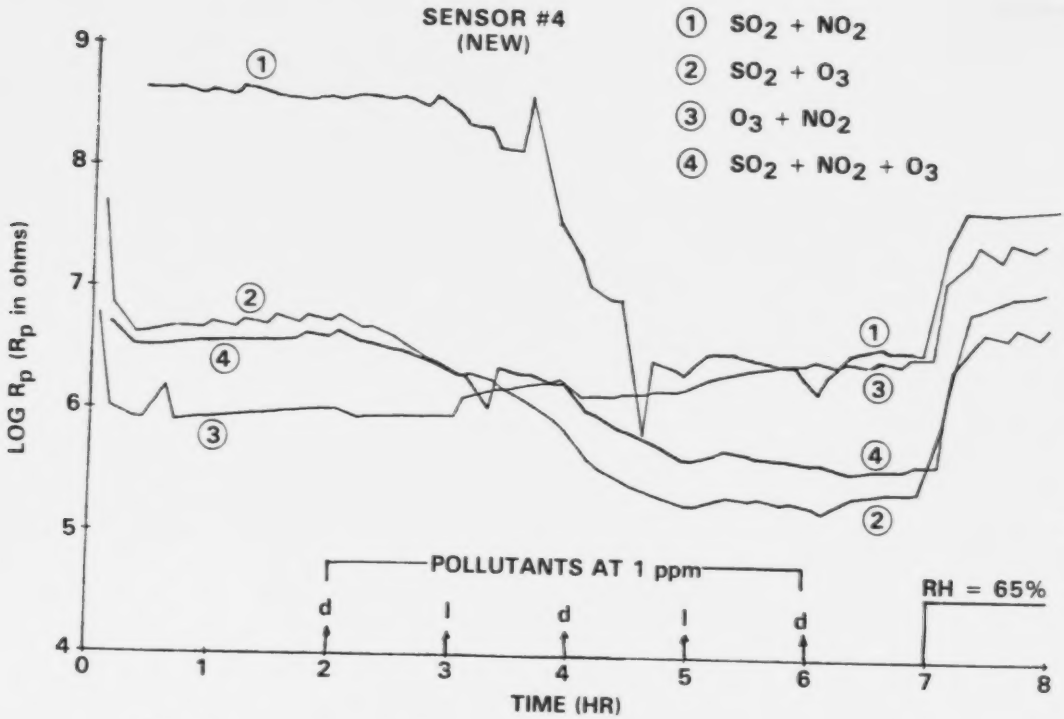

Fig. 10 Response of Sensor No. 4 to four different combinations of pollutants and UV light.

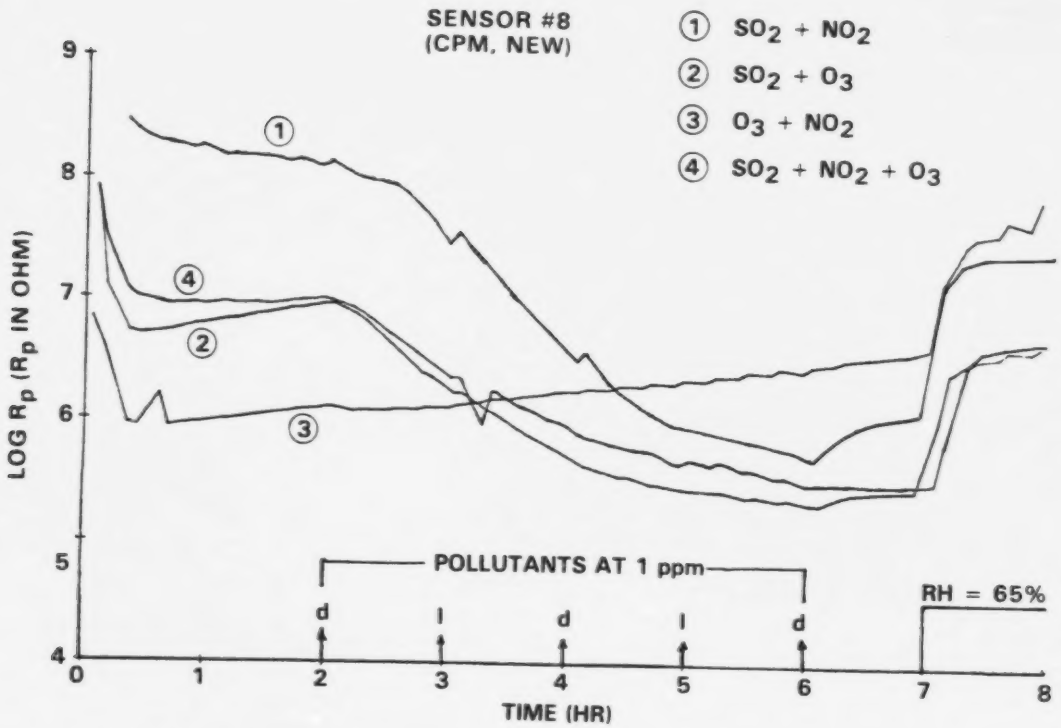

Fig. 11 Response of Sensor No. 8 to four different combinations of pollutants and UV light.

In the first exposure period (SO_2 + NO_2 (Fig. 9)) all sensors showed very small currents until the pollutants were introduced. The current increased continuously until the pollutants were turned off. A very big change occurred when RH was reduced to 65%. After the night at RH = 65% the test was repeated with SO_2 + O_3 (Fig. 10). Apparently the sensors were still activated from the previous test, because the polarization resistance R_p was still low. Introduction of the pollutants led to a continuous decrease of R_p and a slight increase when the pollutants were turned off. A very different response is seen in the present of O_3 + NO_2, where R_p increases continuously.

Apparently in this case the passivating effects of O_3 is stronger than the activating effect of NO_2 which was found in the previous test series. One can also see that the activating effect of SO_2 is stronger than the passivating effect of O_3 (run No. 2). Finally, when all three pollutants are present (run No. 4), an acceleration of corrosion is seen for all sensors.

Integration of the $1/R_p$-time curves for the time period when pollutants were present gave the integrated corrosion loss shown in Table III. The polarization resistance R_p was still very high with a minimum of about 10^5 ohm. Corrosion losses were therefore fairly small and the variations in the three sensor groups fairly large. The highest corrosion loss occurred for series No. 1 and 2 which had been used in test series No. 1 and had been exposed to CPM. However, sensor No. 3 which had not been used before and had not been exposed to CPM, had a corrosion loss which was very similar to that of sensor No. 1. A comparison of sensors Nos. 3-5 with Nos. 6-8 is not very conclusive. It could suggest that CPM lowers corrosion rates slightly as found from analysis of the data in Table II. This is surprising since graphite in its metallic form is expected to accelerate corrosion of zinc by establishment of a galvanic cell. It is possible, however, that such "local action cells" cannot be measured by ACRMs.

Table III

Integrated Corrosion Loss* (in 10^{-2} s/Ω) for the Eight Sensors of Test Series No. 2

Sensor No.	$SO_2 + NO_2$	$SO_2 + O_3$	$O_3 + NO_2$	$SO_2 + NO_2 + O_3$	Total
1 (CPM, No. 1)	2.23	8.10	4.01	4.90	19.24
2 (CPM, No. 1)	3.35	11.92	6.31	6.79	28.37
3	1.85	8.25	4.07	6.46	20.63
4	0.24	3.62	1.03	1.73	6.62
5	0.83	5.30	1.86	4.00	11.99
6 (CPM)	1.58	5.31	1.34	2.66	10.89
7 (CPM)	0.34	2.05	0.48	1.55	4.42
8 (CPM)	0.83	2.95	0.86	1.90	6.54
M	1.41	5.94	2.50	3.75	
SD	1.06	3.30	2.07	2.12	
V	0.98	9.50	3.74	3.94	

*Integrated for t = 2 - 6 h when pollutants were present
All sensors have $CaCl_2$ pretreatment

The main conclusions from this test series are: (1) corrosion rates are very low in the absence of visible electrolyte layers, (2) there are no significant differences of corrosion rates for the four different combinations of pollutants and (3) there is no obvious effect of UV light. It should be pointed out that these conclusions are only valid for this type of exposure when surface electrolyte is formed by condensation of water from the test atmosphere. In the case of "rain" as simulated in the next series, the effects might be more pronounced.

3.3 Effect of Exposure to Pollutants, Simulated Rain Cycles and UV Light

In the third test series eight sensors of different history were exposed to all three pollutants with cooling and warming of the sensors to simulate rain cycles and exposure to UV light during the drying cycles.

The eight sensors were first exposed to RH = 90% for 2 h in the presence of SO_2 + NO_2 + O_3 at 1 ppm each. The sensors were then cooled for 2 h, which led to condensation, followed by 2 h at room temperature in the presence of UV light. The pollutant flow was then stopped. After the first day the ACRMs were exposed overnight at RH = 90%, while after the second day they were kept at RH = 45%. Before the first test all eight sensors were put through the RH cycle. Sensors Nos. 1-6 had been used before in test series Nos. 1 and 2, while Nos. 5-8 were new (see Table IV). All sensors had $CaCl_2$ pretreatment. Sensors Nos. 1, 2, 3, 5, and 6 were covered with CPM.

Table IV

Integrated Corrosion Loss for Test Series No. 3 (s/Ω)

Sensor No.	1	2	3	4
1	1.35	0.99	1.16	3.50
2	0.89	0.80	0.95	2.64
3	1.90	1.85	1.86	5.61
4	1.18	0.63	0.69	2.50
5	1.85	0.98	1.24	4.07
6	1.45	0.27	0.51	2.23
7	0.56	0.19	0.06	0.81
8	0.022	0.014	0.031	0.067

	Sensor History	
Sensor No.	CPM	Previous Tests Series
1	+	Nos. 1, 2
2	+	Nos. 1, 2
3	+	No. 2
4	-	No. 2
5	+	--
6	+	--
7	-	--
8	-	--

Examples for the experimental results for four sensors are shown in Fig. 12a-c for the three days of testing. Cooling of the sensors leads to an almost instantaneous dip of R_p. On the first day (Fig. 12a) corrosion current increased by more than a factor of 50. It is interesting to note that R_p increases again slightly during further cooling and decreases again during warming under UV light. It is also important to note that on the first day, R_p increased only 0.5 h after the pollutants were turned off, while on the second and third day there was an immediate response. The increase of corrosion currents during warming in the presence of UV light could be due to the UV light, since one could assume that the corrosion currents would decrease when the sensor surface temperature is raised. This observed increase of the corrosion current is also noteworthy in light of the further decrease of the SO_2 concentration at the outlet of this test cell. The SO_2 concentration decreases immediately when surface electrolyte is formed during cooling in which the SO_2 dissolves. RH decreases due to condensation on the cold surface and increases again when the surface is warmed.

The different history of the sensors is not clearly reflected in the corrosion behavior for the first day, but for the second and third day sensors Nos. 1 and 3, which had been exposed before, had higher corrosion rates at RH = 90%. When condensation occurs, sensor No. 5 behaves similar to Nos. 1 and 3, while No. 7 corrodes at much lower rates. When the data are analyzed for the effects of successive exposure, it appears that the largest effects are found for the time period at RH = 90%. After exposure overnight to RH = 90% there is a large difference in R_p for the four sensors. After exposure overnight at RH = 45%, this difference becomes more pronounced between sensor No. 7 and the other three sensors. During the cool and warm periods the corrosion rates for sensors Nos. 1, 3 and 5 are very similar and more or less the same for the three days of testing. The reason for the continuous decrease of corrosion rates for sensor No. 7 is not clear.

The corrosion damage for each sensor as determined by integration of the R_p^{-1}-time curves is listed in Table IV. A comparison of the corrosion data

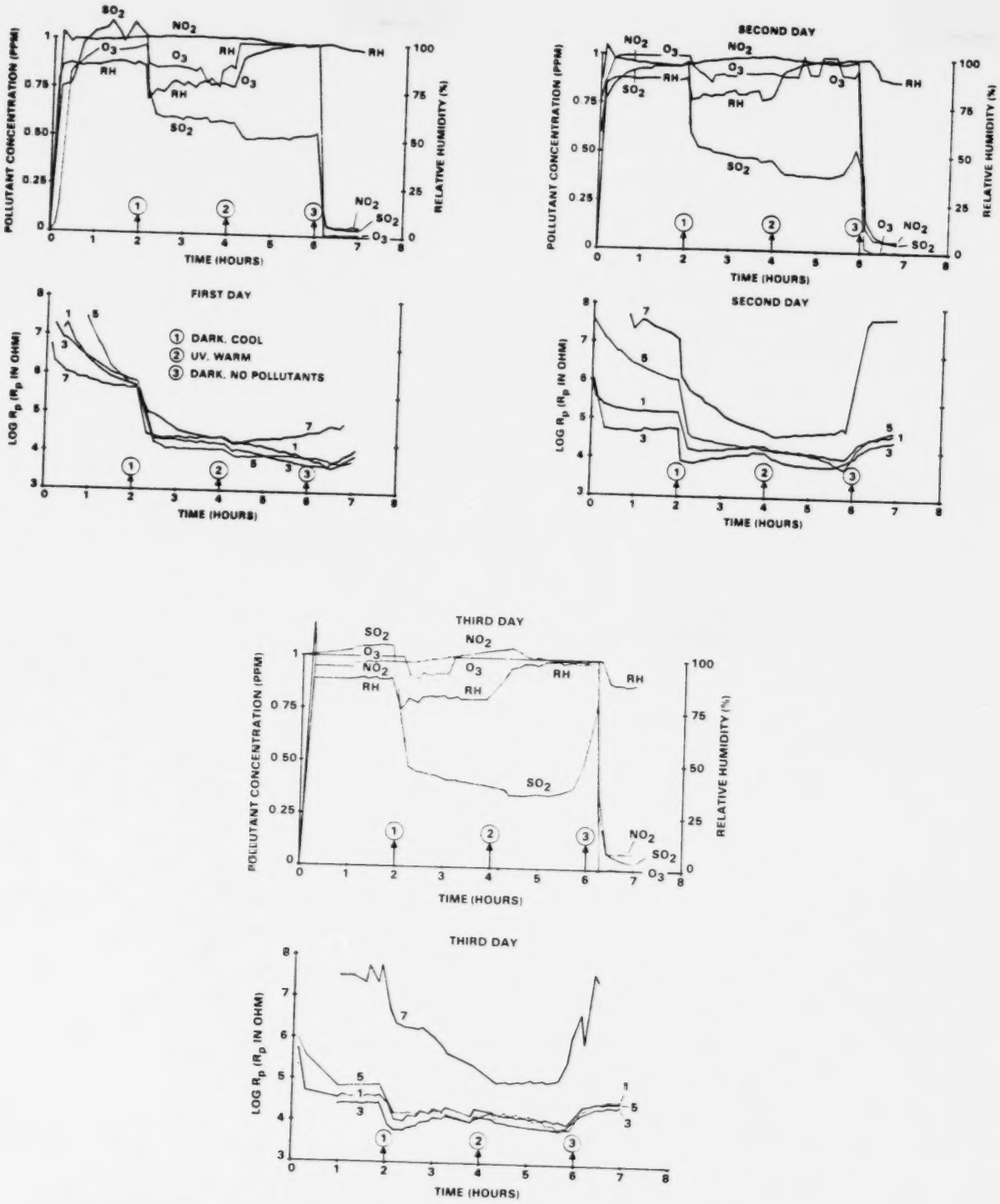

Fig. 12 Pollutant concentration and polarization resistance R_p as a function of time and environmental conditions for four sensors exposed on three successive days.

for a given sensor for the three tests shows that a minimum occurred on the second day. A closer analysis of the corresponding RH and pollutant data would be necessary to determine the cause of this effect. When the different sensors are compared, it becomes clear that the absence of particulate matter reduces the response of a sensor (Nos. 7 and 8). Previous exposure does not seem to change the response to a given environment very much as can be seen from a comparison of the corrosion damage for sensors Nos. 1, 2 and 3 with sensors Nos. 5 and 6. Sensor No. 4 which did not have CPM, but was exposed previously in the series No. 2, has a corrosion damage comparable to that of sensors Nos. 2 and 6.

3.4 Effect of Exposure of Pollutants and Aerosols

The experiments with H_2SO_4 and acetic acid aerosols were each run over a two-day period. A total of 8 new sensors was used in each test. The test procedure was as follows (see also Figs. 13 and 14).

On the first day four sensors, which were pretreated with $CaCl_2$, were exposed for 1 h at RH = 90%, followed by 2 h at RH = 90% in the presence of the aerosol. Four new sensors were then added and after 1 h at RH = 90% the aerosol and O_3, SO_2 and NO_2 at 1 ppm each were added to the test cell for 2 h. After this the flow of aerosol and pollutants was stopped and RH = 90% maintained for 1 h, followed by RH = 65% overnight.

For the second day the same sequence of events was followed except that all 8 sensors were run at the same time.

In Fig. 13a and b examples are given for both tests. In Fig 13a, No. 3,1 refers to sensor No. 3 on the first day, while No. 3,2 indicates the data for the same sensor on the second day.

In Fig. 13a, the polarization resistance R_p data show the accelerating effect of the H_2SO_4 aerosol in the first hours of the test when the aerosol is added and removed from the test atmosphere. After exposure to aerosol and pollutants the sensor output does not change much when the aerosol and

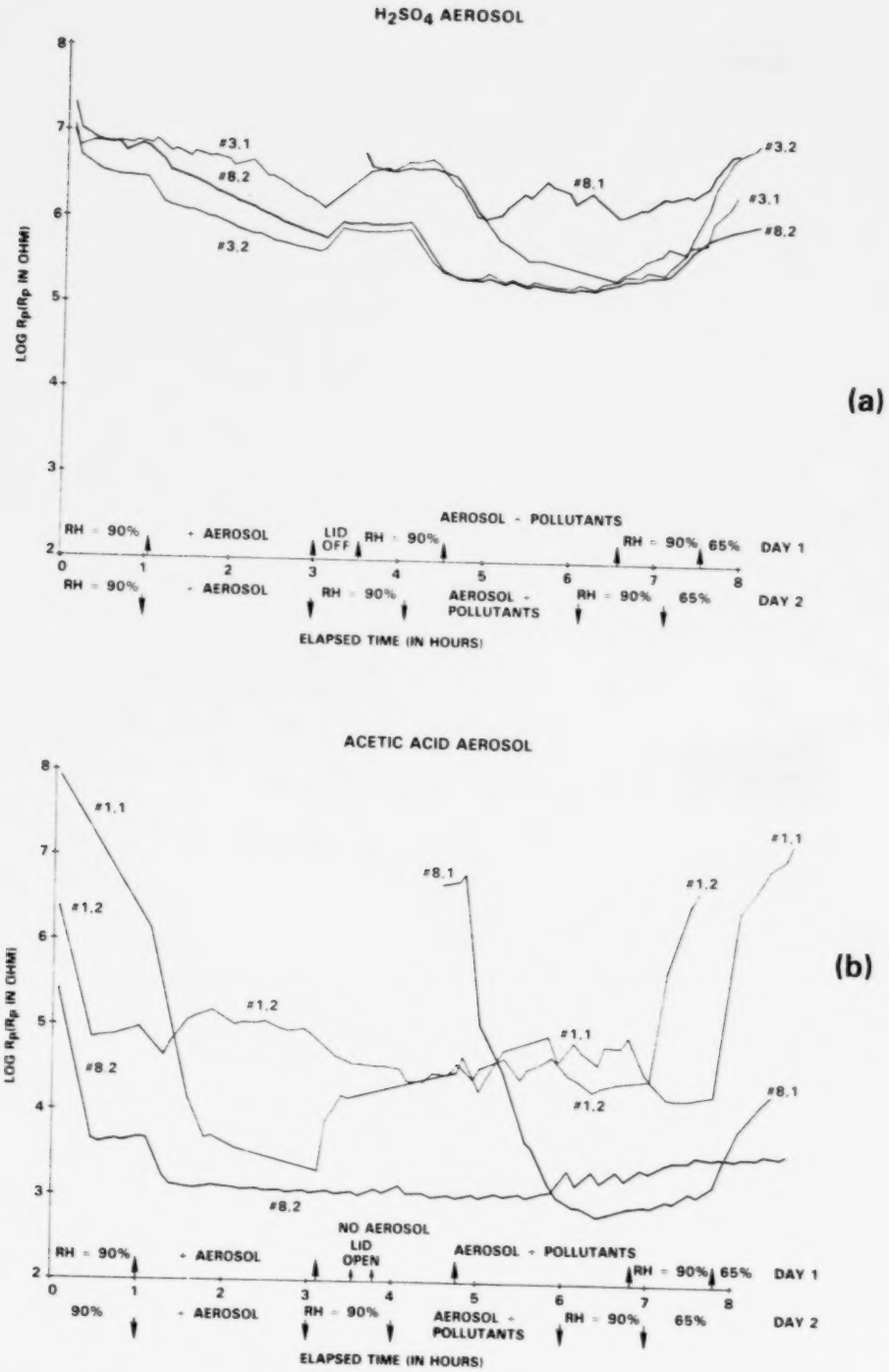

Fig. 13 Polarization resistance R_p during exposure to H_2SO_4 aerosol (Fig. 13a) and acetic acid aerosol (Fig. 13b) with and without presence of pollutants.

pollutant flow is stopped, especially on the second day. Sensor No. 8,1 shows some unexpected behavior since its corrosion rate seems to decrease when aerosols and pollutants were added. The other three sensors, which were added to the second half of this test, show the expected increase of corrosion rates in the presence of aerosol and pollutants and a decrease upon their removal from the test atmosphere.

Much higher corrosion rates were observed in the presence of the acetic acid aerosol (Fig. 13b). Since the acetic acid is volatile, it is considered to dissolve in the surface electrolyte formed on the sensor surface at higher RH. The sensors, which were added in the first or the second half of the test on the first day, showed steep drops of R_p upon introduction of the aerosol. Sensor No. 1 did not, however, show a decrease of R_p when aerosols and pollutants were present. On the second day R_p was very low for all sensors and did not change much with environmental conditions. It was observed that salt crystals had grown between the fingers of the sensors which could shorten the sensors (Fig. 14). The ACRM in Fig. 14 had been coated with CPM.

Table V gives a summary of the integrated corrosion loss data for both tests. On the first day, sensors Nos. 1-4 were exposed throughout the whole test duration, while sensors Nos. 5-8 were exposed only in the second half of the test. For the exposure to H_2SO_4 aerosol, higher corrosion losses were observed for the second day, while the opposite behavior was observed for the acetic acid aerosol except for sensors Nos. 6 and 8 which had very high corrosion currents. It is possible that the low observed R_p-values are due to the shorting of the sensors.

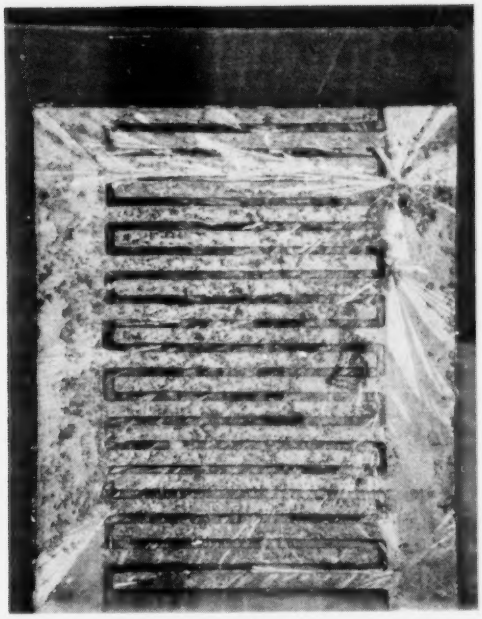

(a)

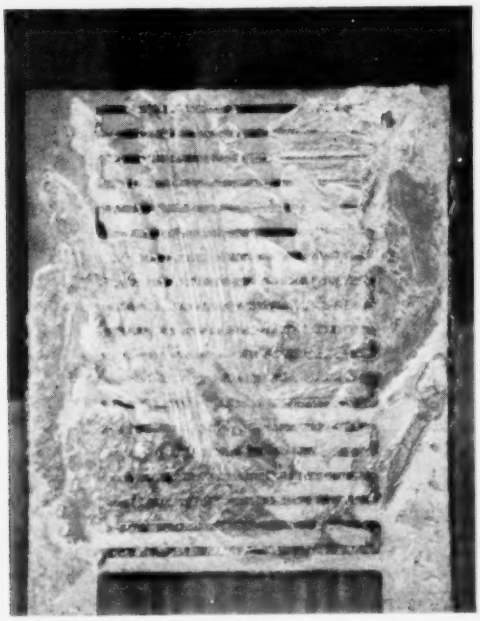

(b)

Fig. 14 Photograph of two sensors after exposure to acetic acid aerosol.

Table V

Corrosion Loss (s/Ω) for Zinc ACRMs

Sensor No.	First Day	Second Day
	H_2SO_4 Aerosol	
1	0.015*	0.051
2	0.044*	0.079
3	0.031	0.069
4	0.041	0.078
5	0.005*	0.029
6	0.020*	0.110
7	0.019	0.068
8	0.007	0.068
	Acetic Acid Aerosol	
1	2.28*	0.55
2	0.76*	0.49
3	0.67	0.56
4	16.88	0.35
5	10.73*	0.13
6	12.99*	30.75
7	1.17	0.51
8	8.54	17.24

*Covered with carbon particulate matter.

4.0 DESIGN AND TEST OF THE DATA LOGGING SYSTEM (ACRMDL) (TASK II)

The Atmospheric Corrosion Rate Meter and Data Logger (ACRMDL) has been designed and constructed by Prof. D.K. Roe under a subcontract. The ACRMDL is used for control of the ACRMs and data collection. It incorporates a small computer programmed in Basic language which has sufficient memory to log 4,608 measurements from six sensors over a four-day period. A printer/plotter is used to provide hard copies of the results as log R_p vs time in tabular and graphical form. Results may also be transferred to cassette tape or to another computer via an RS-232C interface.

The specifications and operational characteristics of the ACRMDL are described in Appendix II, which also contains ACMDA, the Atmospheric Corrosion Monitor and Data Acquisition Program. An additional computer program has been prepared by Science Center personnel for transfer of the experimental data from the ACRMDA to the VAX 11/780 computer for storage and further processing (analysis, display) of the data. This data transfer is also necessary since only a limited amount of data can be stored on the ACRMDL. It also prevents accidental loss of data.

A typical print-out of a log Z, where Z is the polarization resistance R_p, vs time trace is shown for three sensors in Fig. 15. Contrary to the system used in Task I, which had a larger range, but the disadvantage that the measuring resistor and gains of amplifiers had to be adjusted manually, the ACRMDL allows continuous monitoring of sensor output for the changing environmental conditions in Fig. 15, since log convertors are used for the recording of the current. The results in Fig. 15 clearly show the changes of sensor output with changing atmospheric conditions. Figure 15 was produced with the Radio Shack TR580 model PC-3 computer and plotter interface which are part of the ACRMDL (see Appendix II).

An additional modification of Prof. Roe's program was made to obtain integration of the sensor data using the PC-3 computer before transfer of the data to the VAX 11/780 computer.

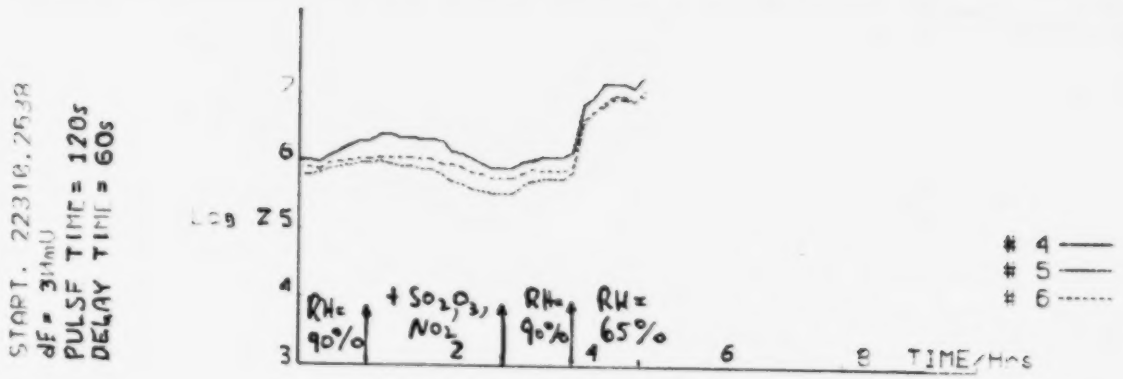

Fig. 15 Plot of ACRM data for three sensors as recorded with ACRMDL.

As part of the test of the ACRMDL, the reproducibility of R_p-measurements was evaluated for ACRMs which was pretreated with DI water and for ACRMs without pretreatment (three sensors each). The measurement was repeated for four 8 h cycles with RH = 65% overnight. Figure 16 shows the response for the four cycles of one sensor for each of the two pretreatments. The environmental parameters are also given. The integrated corrosion loss is listed in Table VI. Figure 16 and Table VI show that, as expected, there is a much higher corrosion loss for the H_2O treatment. In both cases the corrosion loss becomes less for subsequent cycles.

Tale VI

Integrated Corrosion Loss (s/Ω) for Six ACRMs During a Four Day Cycle of RH and Pollutants

Sensor No.	PT	Day 1	2	3	4	Mean
1	H_2O	0.225	0.302	0.298	0.327	0.288
2	H_2O	0.271	0.216	0.0734	0.0459	0.152
3	H_2O	0.224	0.375	0.220	0.0821	0.225
4	-	0.0453	0.00497	0.00259	0.00097	0.0135
5	-	0.0146	0.0407	0.00604	0.0014	0.0157
6	-	n.d.	0.0669	0.0583	0.0645	0.0632

n.d. = no data

In another test series the effect of NO_2 on the corrosion losses determined by ACRMs was determined. The sensors were first exposed at RH = 90% for 1 h, 1 ppm NO_2 was then added for 4 h, followed by 1 h at RH = 90% without NO_2 and RH = 65% overnight. This cycle was carried out in the same manner for four days. No clear effect of NO_2 could be detected. The most obvious result of this test series was the larger corrosion loss for the NaCl pretreatment and the continuing decrease of corrosion rates with the number of cycles (see Table VII). Corrosion losses were much smaller than in the previous test series in which SO_2 and O_3 were used as pollutants (see Table VI). The units in Table VII are 10^{-2} s/Ω compared to s/Ω in Table VI.

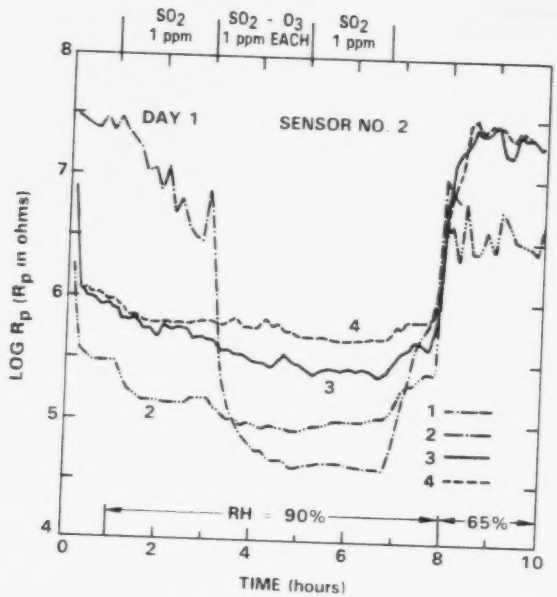

(a)

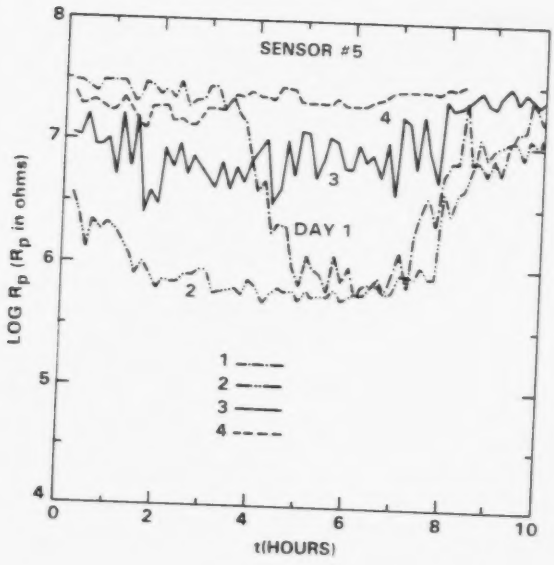

(b)

Fig. 16 Sensor response for changes in environmental conditions for four cycles. Sensor No. 2 has H_2O pretreatment, sensor No. 5 is without pretreatment.

Table VII

Integrated Corrosion Loss for Exposure to NO_2 (10^{-2} s/Ω)

Sensor No.	PT	Day 1	2	3	4
1	NaCl	2.40	1.02	0.849	0.430
2	NaCl	4.58	2.61	1.79	0.958
3	NaCl	4.92	1.64	1.33	0.509
4	$CaCl_2$	1.64	0.478	0.436	0.359
5	$CaCl_2$	1.31	0.533	0.505	0.330
6	$CaCl_2$	1.07	0.482	0.486	0.337

In order to check the procedure for the exposure test in Task III and the response of the ACRMs, an additional test series was performed in which RH was kept at 95% for 7 h followed by RH = 65% overnight. After 1 h at RH = 95% the base plate of the test cell to which the sensor was attached was cooled 3°C vs room temperature except on the first day where it was 4°C. Cooling was maintained for 5 h. Two hours after start of the test SO_2 was introduced at 0.5 ppm for 1 h, followed by 1 ppm for 1 h and 0.5 ppm for 1 h. The SO_2 was then turned off. This cycle was carried out for 5 days. Figure 17 gives an example for four sensors with different pretreatment for the first and fourth day. Table VIII summarizes the results for this test. In Fig. 17 the inverse polarization resistance $1/R_p$ is plotted which is directly proportional to the corrosion rate of the ACRM. This type of plot shows the changes of corrosion rates during periods of accelerated corrosion more clearly than the log R_p-plot, while the corrosion behavior during the periods of low corrosion activity cannot be recognized too well.

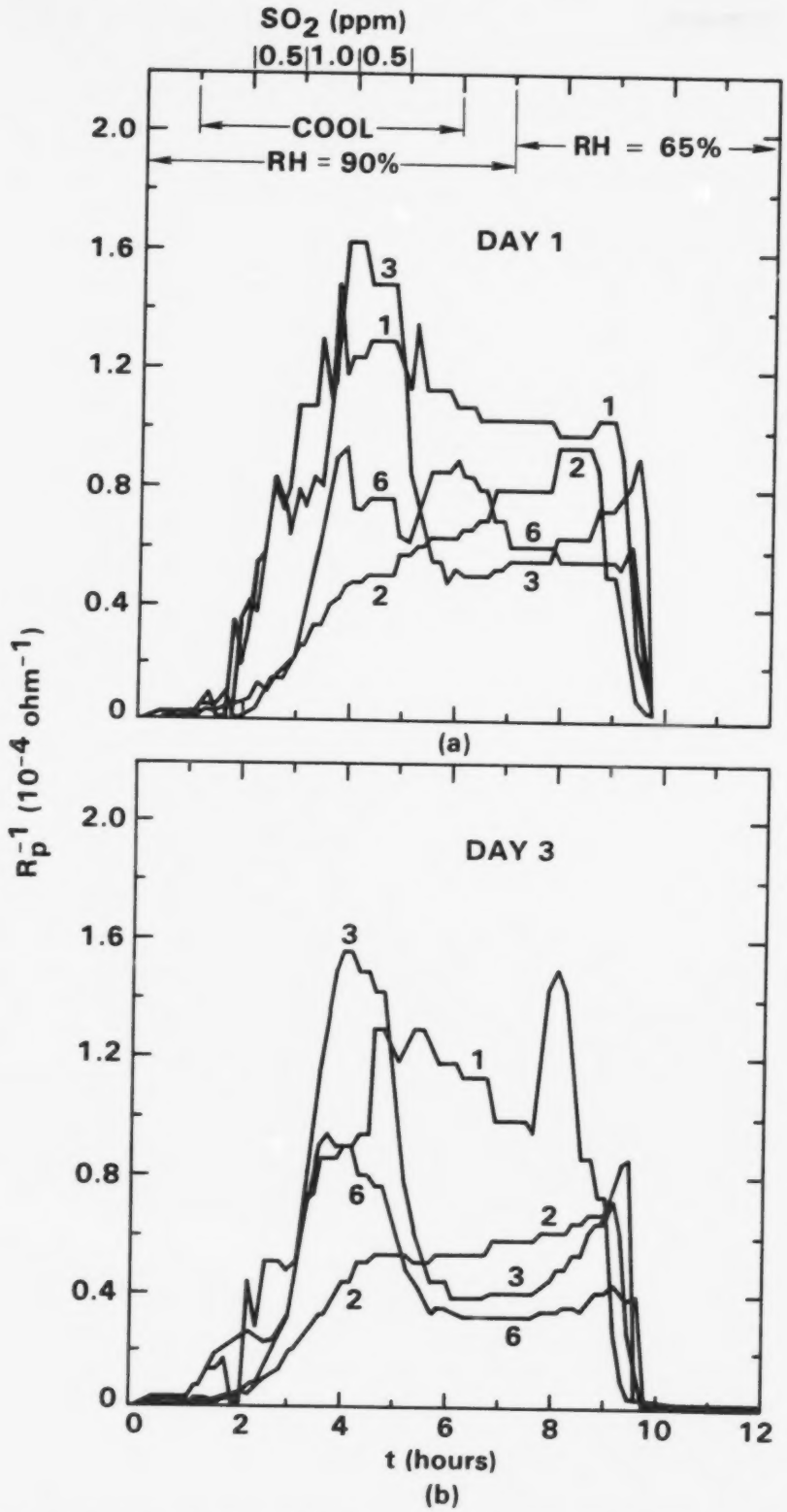

Fig. 17 Response of four ACRMs with different pretreatments to changes in environmental conditions.

Table VIII

Integrated Corrosion Loss (s/Ω) for Exposure to SO_2 During Cooling

Sensor No.	PT	Day 1	2	3	4	5*	Mean
1	NaCl	2.79	2.35	2.47	4.95	2.67	3.05
2	$CaCl_2$	1.49	0.62	1.25	0.88	1.13	1.07
3	H_2O	2.22	2.00	1.88	1.56	1.89	1.91
4	H_2O	1.52	0.68	0.97	0.90	1.02	1.02
5	-	3.06	1.41	1.71	1.40	1.65	1.85
6	-	1.62	1.57	1.23	1.02	1.14	1.32

*t = 7-8 h at RH = 95%

5.0 CORRELATION OF SENSOR RESPONSE WITH DETERIORATION OF DIFFERENT MATERIALS (TASK III)

The purpose of this task was to determine whether the response of the new zinc ACRM can be used as a proxy for the deterioration rate of other materials. This question was answered by determining the corrosion behavior of weathering steel, galvanized steel, marble, latex house paint and oil base house paint (on stainless steel) by the weight loss method. The corrosion behavior of these materials in outdoor exposure had been determined earlier in the St. Louis Study (14,15). An ACRM was attached to the surface of one of the triplicate materials, and the ACRM output was recorded continuously with the ACRMDL.

The experiment was conducted in a special test cell which allowed the interaction of the pollutants and cooling of the exposed samples which were coated with a polymer coating on their back and attached vertically to the test cell wall. After the 31 day test, the weight loss determined using specific solutions and taking into account the weight loss of a blank. The weathering steel had developed a very uniform layer of corrosion products.

The exposure test consisted of a cooling-warming cycle of 1.5 h cooling followed by 4.5 h at a higher temperature as shown in Fig. 18 for a 26 h period. When the temperature was reduced, the SO_2 concentration, as measured at the outlet of the test cell, dropped due to dissolution of the SO_2 in the surface electrolyte. Also shown in Fig. 18 is the RH as calculated from the temperature of the test cell and the dew point of the air coming out of the test cell. The ACRM response (Fig. 18) follows closely this cycle of environmental conditions. In the first cycle R_p changes by a factor of two between the "cool" and the "warm" condition of the ACRM attached to one of the specimen. Figure 19 shows an 80 h cycle in the early and middle part of the test period, respectively, for the six ACRMs. The cyclic response of the ACRMs is clearly seen in both figures. Between 70 and 150 h exposure time there is a gradual decrease of R_p corresponding to a slow increase of

corrosion rates, while between 310 and 380 h the high and low values in a given cycle do not change much with time. It becomes apparent that sensors Nos. 1, 2, 5 and 6 show very similar values of R_p, while sensors Nos. 3 and 4 have higher values which are more or less the same for these two sensors. These differences can be traced back to the different portions of the ACRMs in the test cell. Sensors Nos. 1 and 2 were located on the west wall of the cell, while sensors Nos. 5 and 6 were on the opposite east wall in an equivalent position. The sensors Nos. 3 and 4 were located next to each other on the south wall. Figure 20 gives a schematic of the experiment arrangement for test coupons and ACRMs. Since the air flow came out of the tubes which were parallel to the east and west walls, it is possible that the pollutant and wet air flow was different for these two walls as compared to the south wall.

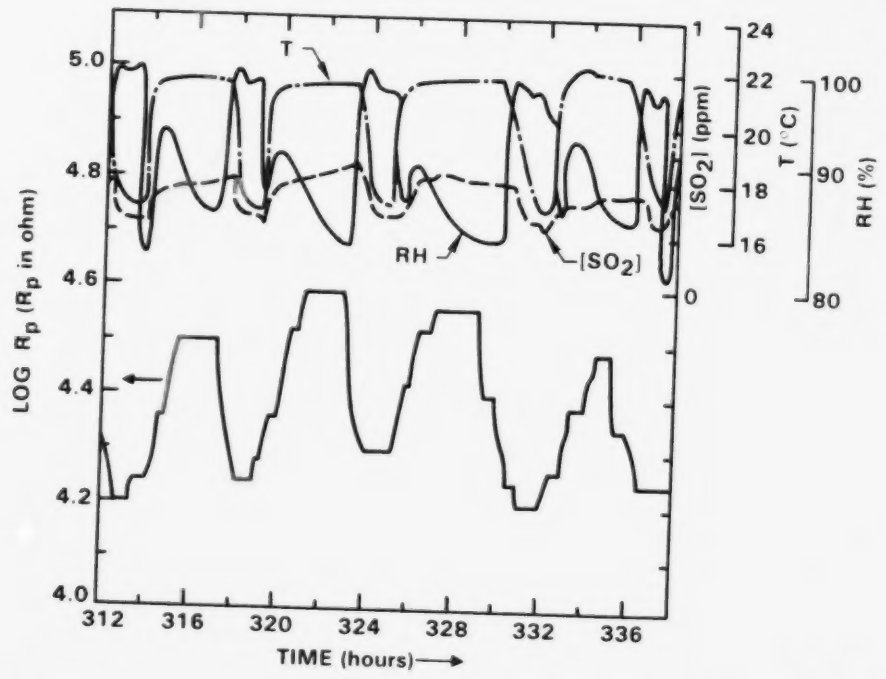

Fig. 18 Environmental changes and response of an ACRM.

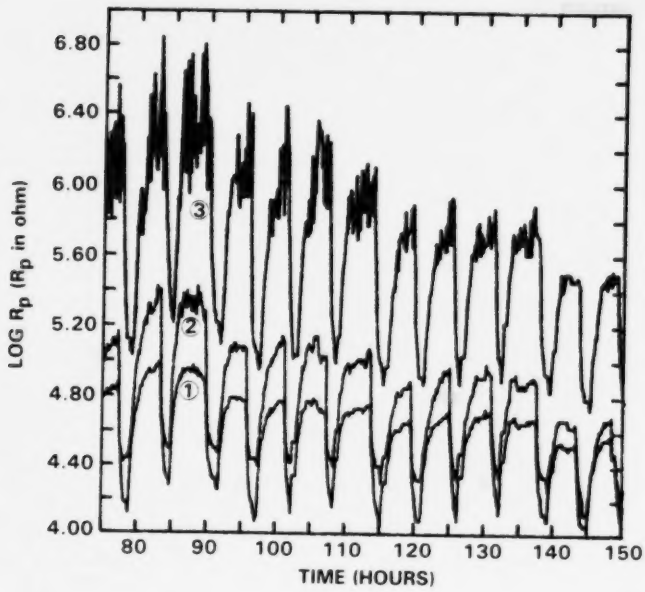

(a)

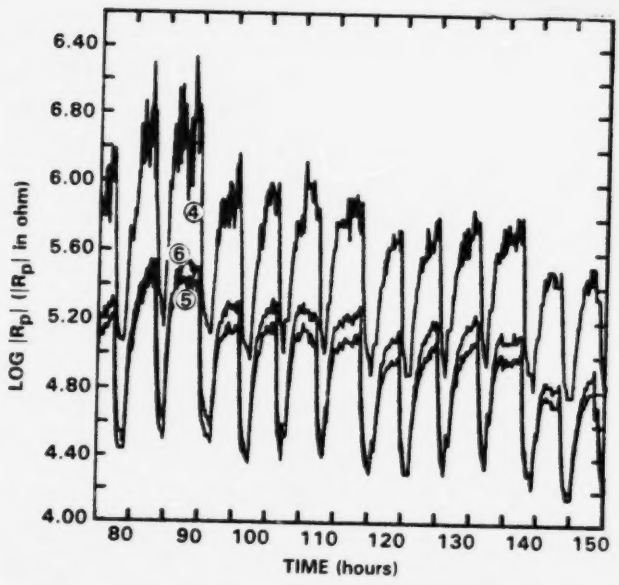

(b)

Fig. 19 Two 80 h test cycles for six ACRMs.

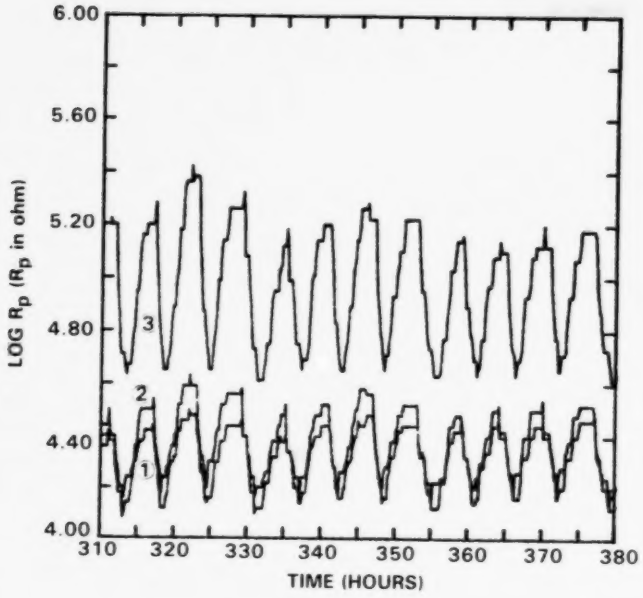

(c)

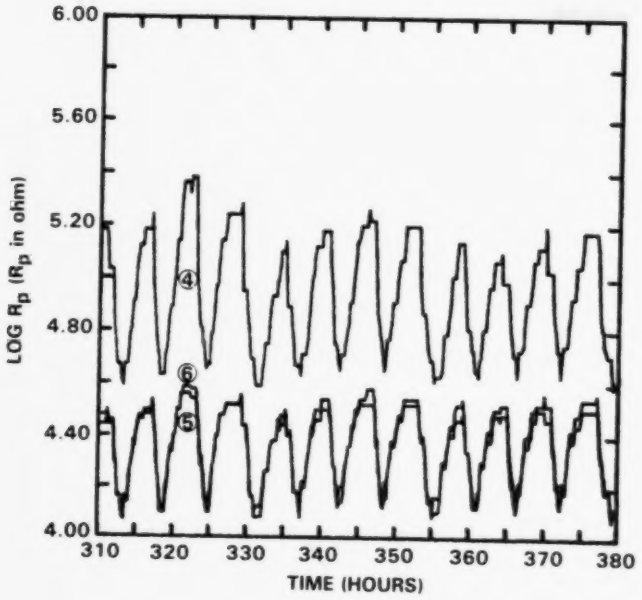

(d)

Fig. 19 Two 80 h test cycles for six ACRMs.

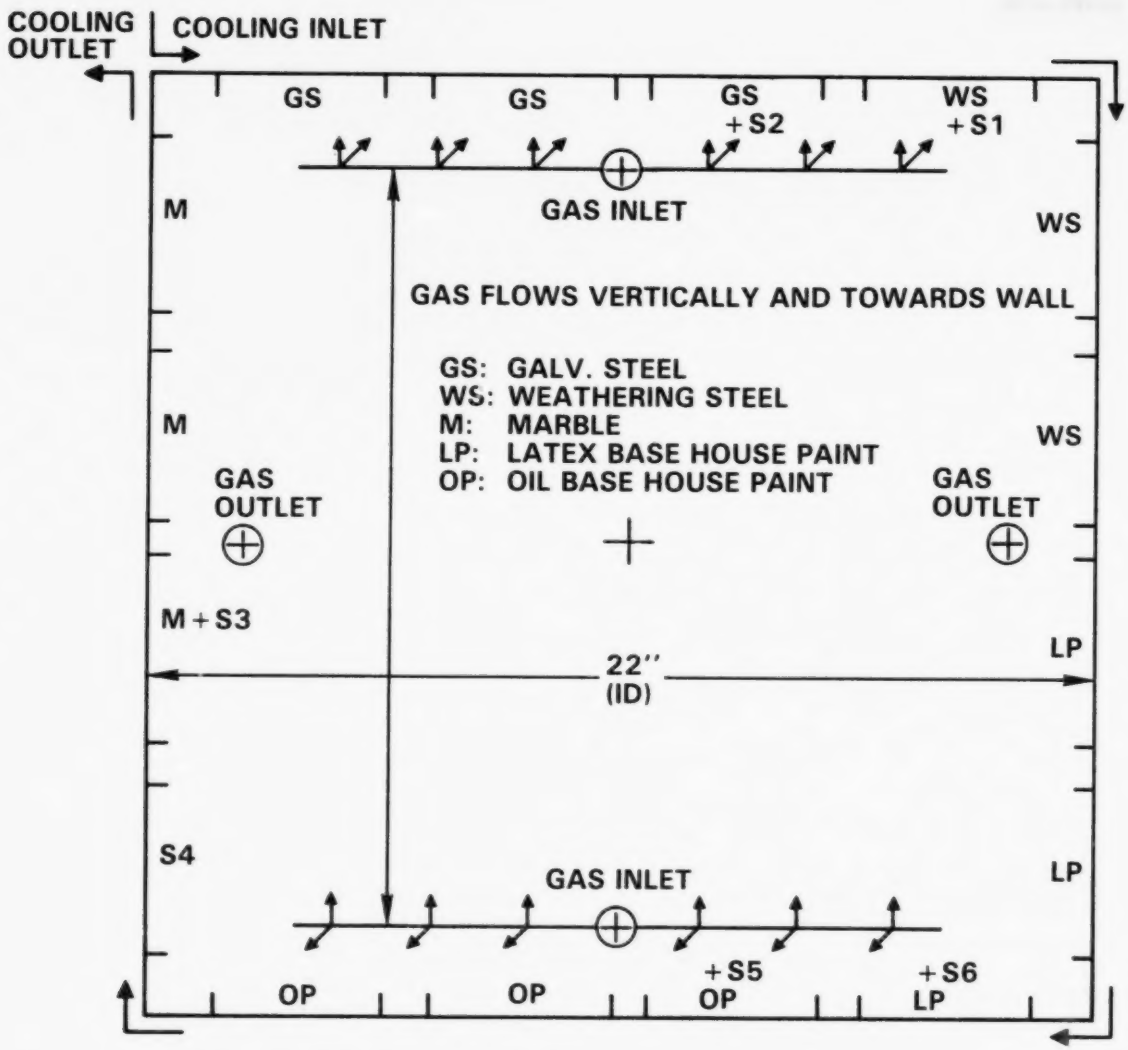

Fig. 20 Schematic of ACRM and test coupon location.

Figure 21 shows the time dependence of the polarization resistance R_p for all six sensors. Figure 22 shows the SO_2 concentration during the dry and wet periods of each cycle and the corresponding maxima and minima of RH. After 31 days RH was reduced to 45% and the SO_2 flow was stopped. ACRM data were recorded in this condition over the weekend. A slow trend to somewhat higher corrosion rates with increasing exposure time was accompanied by a decrease of the difference between high and low values of R_p during a cool-warm cycle. The gap in the data in the beginning of the test is due to a problem with the computer program; the gap around 400 h was caused by a power failure which affected the back-up disk in the VAX computer to which the data had been transferred.

The gradual increase of corrosion rates with exposure time is reflected in Fig. 23 in which the integrated corrosion loss for a given time element (the horizontal bar through the data of sensors No. 1 and 3) is plotted. For sensors Nos. 1, 2, 5 and 6 corrosion losses per time period ($s/\Omega \cdot h$) increase by about a factor of 2 to 3, while for sensors Nos. 3 and 4 this increase is about a factor of 6. However, the corrosion rate at the end of the test is still much less than for the other four sensors.

The weight loss data and the electrochemical data are compared in Table IX. The weight loss of the house paint was found to depend on the RH of the laboratory where the weight was determined. The weight loss data shown in Table IX were, therefore, determined after storage of the coupons in the desiccator. For marble the weight loss was very small and probably within the error of the measurement. For the weathering steel, where a cathodic treatment in H_2SO_4 was used to remove corrosion products, the weight loss was determined by extrapolation to zero descaling time.

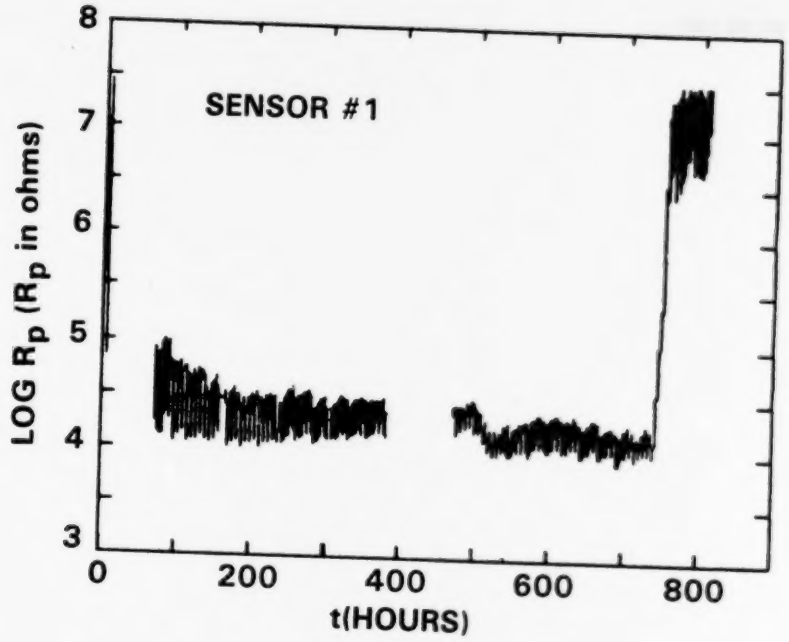

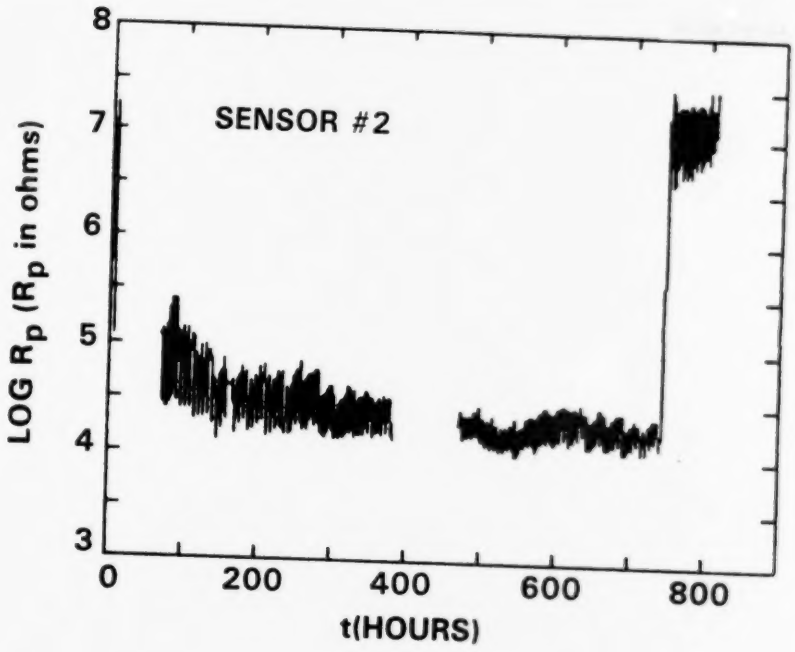

Fig. 21 Time dependence of R_p for six ACRMs during entire test period.

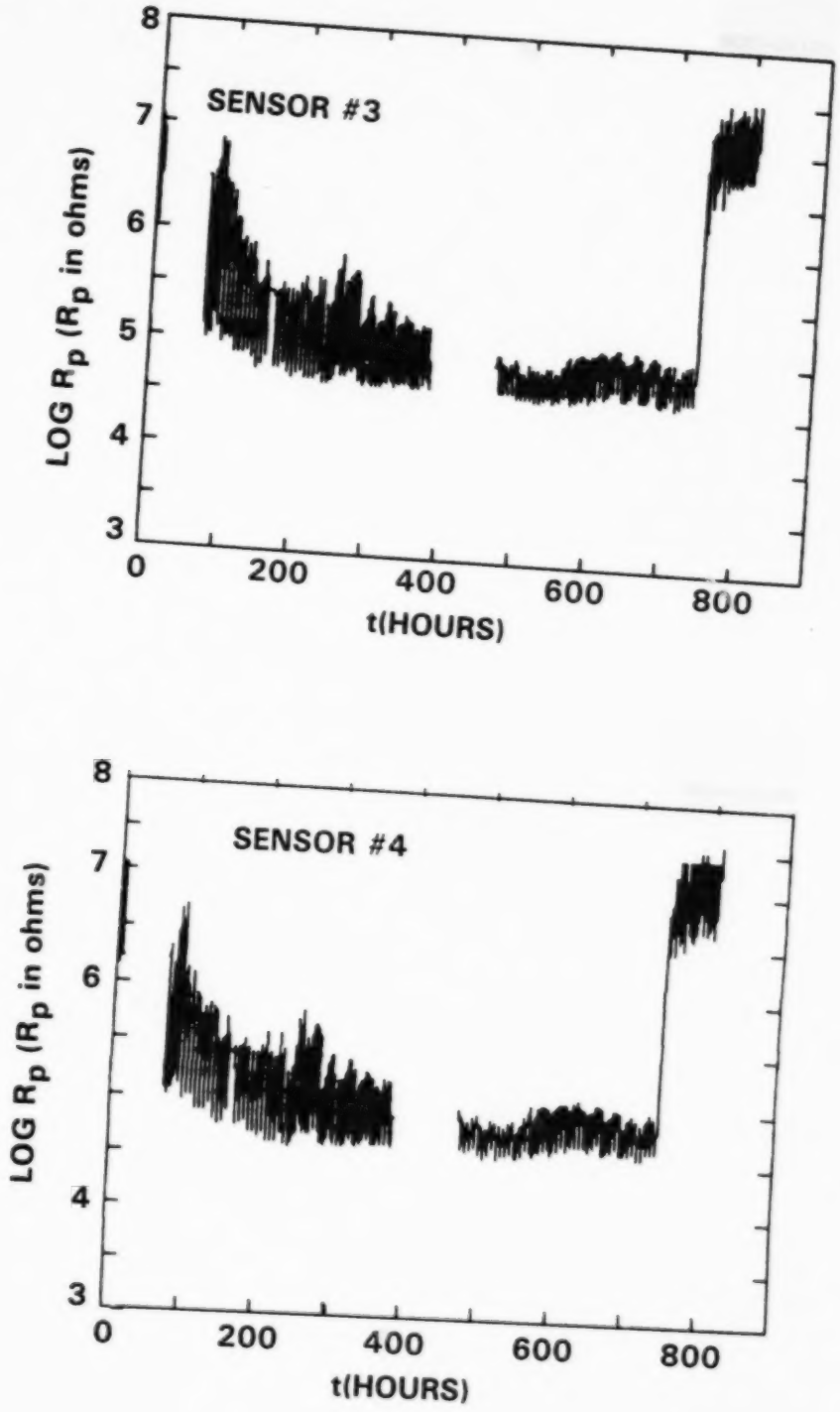

Fig. 21 Time dependence of R_p for six ACRMs during entire test period.

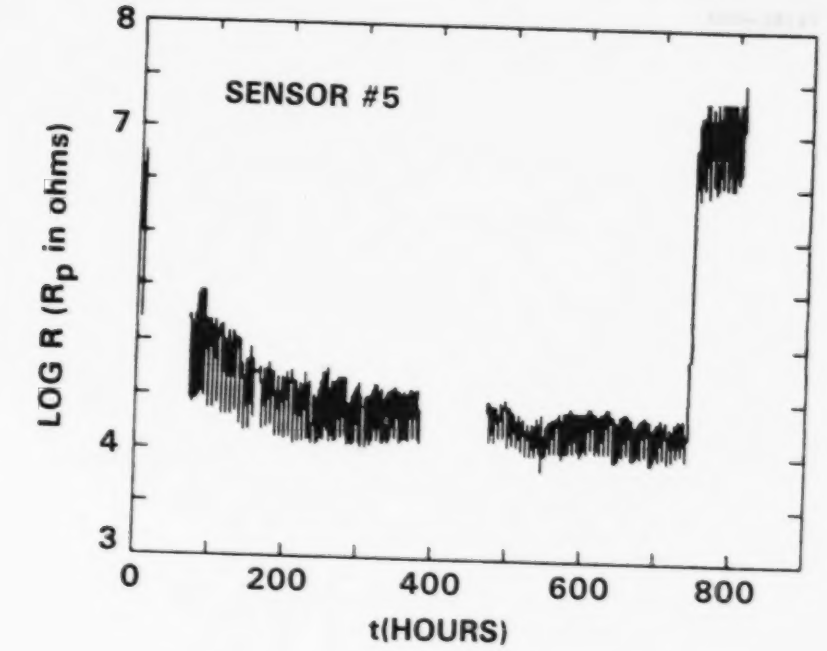

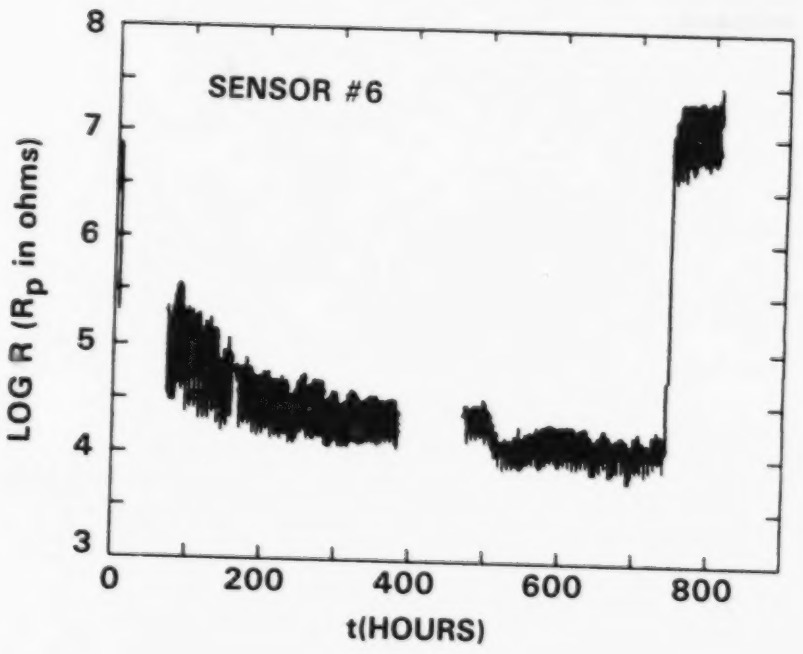

Fig. 21 Time dependence of R_p for six ACRMs during entire test period.

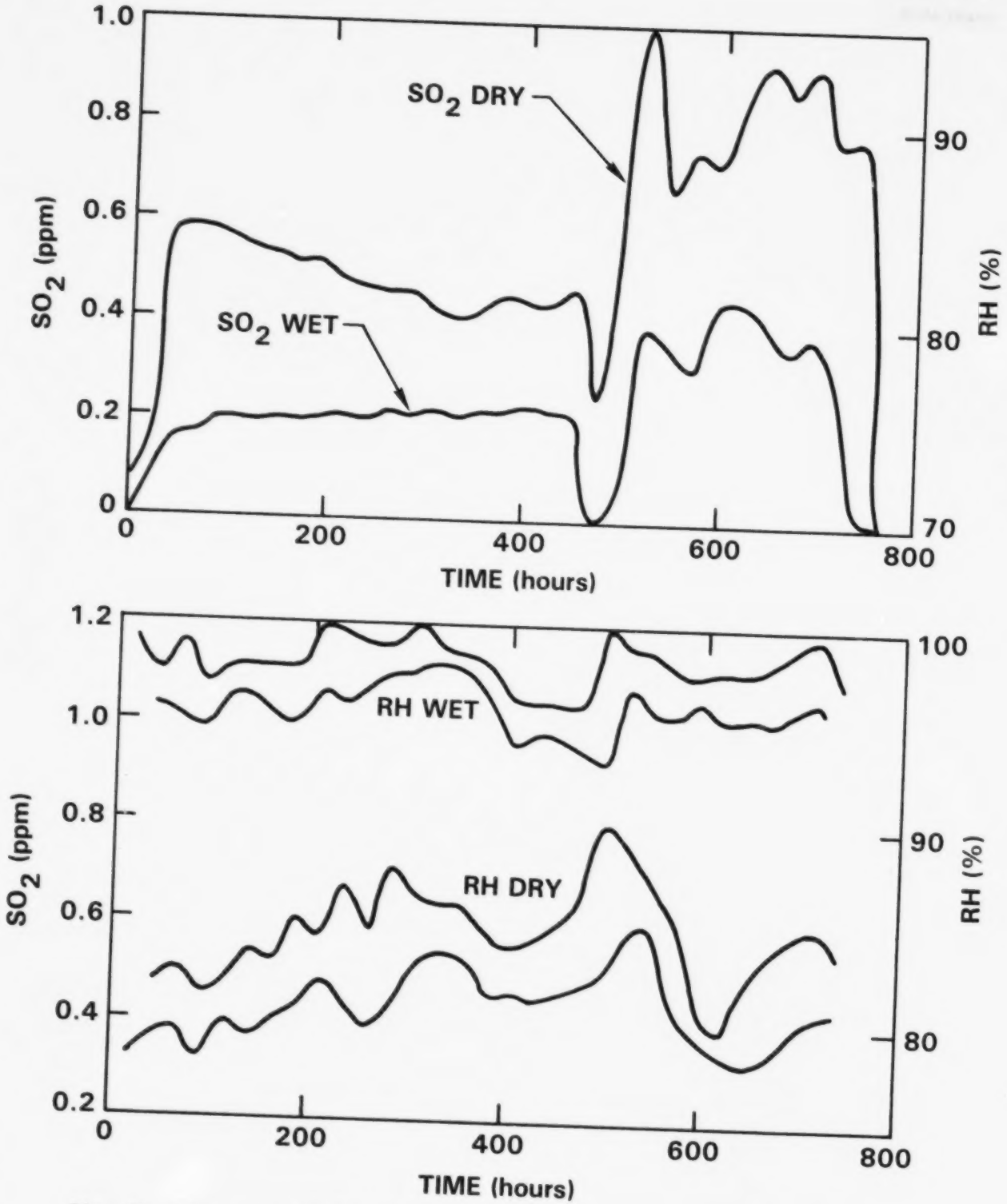

Fig. 22 SO_2 concentration at test cell outlet during "wet" and "dry" periods. Also shown are the corresponding maxima and minima values of RH. The drop of the SO_2-concentration to zero is due to a change to a new tank of SO_2.

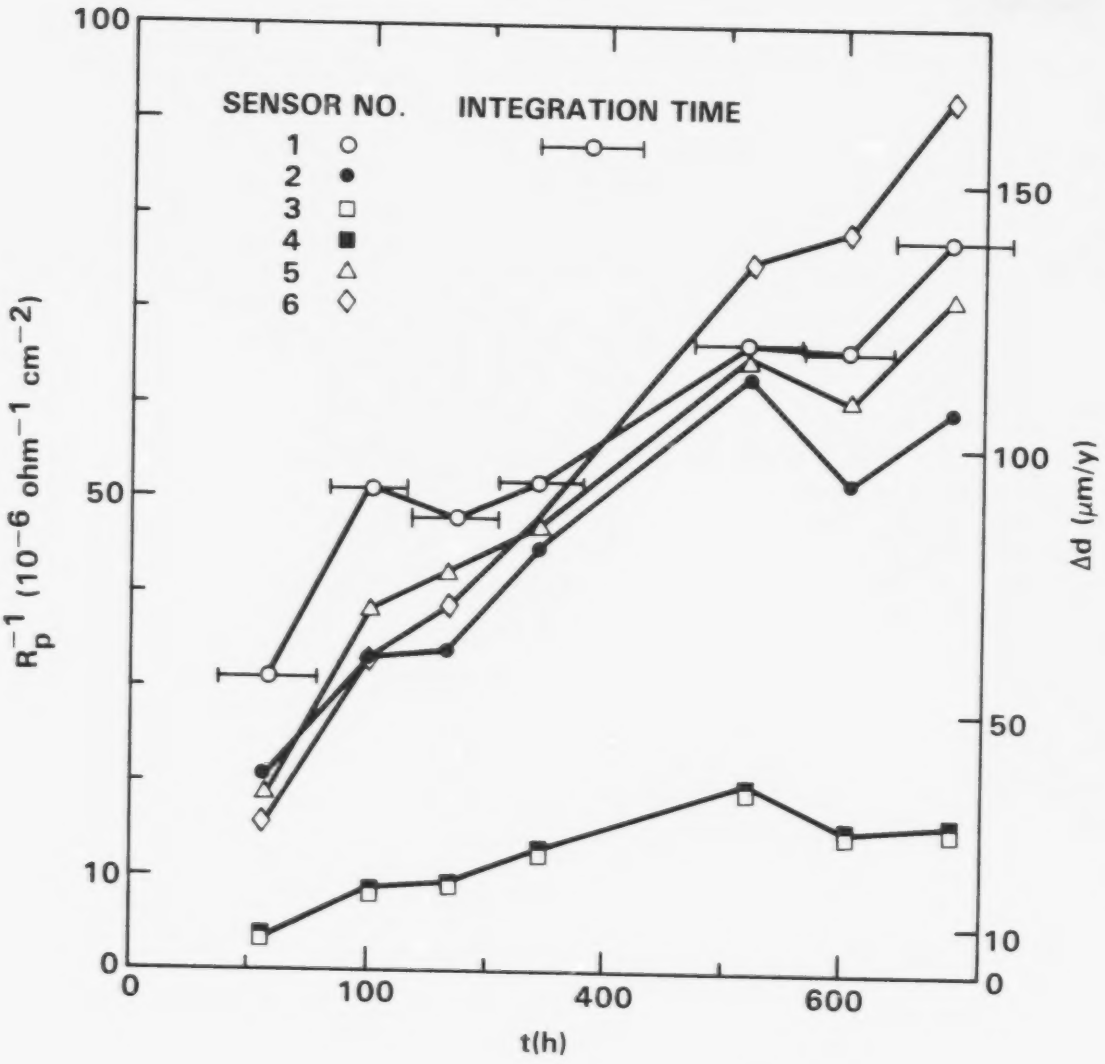

Fig. 23 Integrated corrosion loss of a given time period ("corrosion rate") as a function of exposure time for the six ACRMs.

Table IX

Comparison of Weight Loss and ACRM Data for 31 Day Exposure Test

	Weight Loss (mg/cm^2)	ACRM Data ($s/\Omega \cdot cm^2$)	CF ($mg \cdot \Omega \cdot s^{-1}$)
Galvanized Steel	0.81	71.3	1.14×10^{-2}
Weathering Steel	11.25	90.5	1.24×10^{-1}
Oil Base Paint	0.11	78.1	1.41×10^{-3}
Latex Base Paint	0.07	86.1	8.13×10^{-4}
Marble	(2×10^{-3})	19.2	-
		20.2	

CF = conversion factor

A conversion factor CF has been calculated for galvanized steel, weathering steel and the two house paints as the ratio of the weight loss per unit area of the coupon and the total current flow per unit (active) area of the ACRM which was attached to this coupon. Since the weight loss was very small for the marble, no conversion factor was calculated. Sensors Nos. 3 and 4 were not used in this calculation.

6.0 SUMMARY AND CONCLUSIONS

A new instantaneous atmospheric corrosion rate monitor (ACRM) has been developed and tested. The response of the ACRM to single pollutants and combinations of SO_2, O_3 and NO_2, to aerosols, to diurnal cycles and periods of rain has been characterized. A data logging system - the ACRMDL - has been designed and tested with the ACRM. The ACRMDL is battery operated and can control up to six ACRMs simultaneously. The use of log converters for the recording of the current transients allows accurate meaurements over four decades.

An important question concerning the operation of the ACRMs is the effect of pretreatment on the response of the sensors. A number of experiments have been performed to answer this question. Pretreatments with NaCl, $CaCl_2$ and DI H_2O and with carbonaceous particulate matter have been evaluated. No definite effects could be found in experiments in which the ACRMs were exposed for short time periods without formation of liquid layers, although the absence of pretreatment produced lower corrosion loses. The ACRMs showed, however, almost instantaneous changes of the polarization resistance when RH and the pollutant level, especially of SO_2, were changed. When liquid corrosion layers were formed, especially over long time periods, such as in the exposure test of Task III, the effect of pretreatment was negligible. The sensors are so sensitive in their response to environmental conditions that a less than optimum placement of some sensors in the test cell during the exposure test became quite obvious.

The response of the ACRMs to SO_2, O_3 and NO_2 has been studied as a function of concentration between 0 and 1 ppm. A very pronounced effect of SO_2 and NO_2 concentrations was observed especially when a liquid electrolyte film was present for the ACRM surface. The fact that this effect is reversible shows that the dissolved pollutant does not only change the electrolyte conductivity, but produces as its main effect a change in corrosivity. Aerosols also result in a response from the ACRMs. However, it was found that the

acetic acid aerosols produced conducting corrosion products which shorted out the sensor.

From the results of the exposure test conversion factor have been calculated which can be used to convert ACRM data into corrosion losses of galvanized steel, weathering steel, house paint and marble. It seems desirable to obtain conversion factors also in exposure to natural environments of different corrosivity in order to ascertain the validity of the conversion factors obtained in a laboratory test.

The ACRM in its present form consisting of solid zinc is a very sensitive sensor for the corrosivity of atmospheres and its changes, and for the time-of-wetness. The ACRMDL provides a very convenient way to control the sensor operation and collect the corrosion data. Since it is battery operated, it can be used unattended for long time periods. Data transfer to a larger computer allows analysis and display of the ACRM data in a more detailed manner.

7.0 REFERENCES

1. F. Mansfeld, Proc. 5th European Symp. on Corrosion Inhibition, Ferrara, Italy, 191-216, September 1980.

2. F. Mansfeld, S. Tsai, S. Jeanjaquet, M.E. Meyer, K. Fertig and C. Ogden, "Reproducibility of Electrochemical Measurements of Atmospheric Corrosion Phenomena" ASTM STP 767, 309 (1982).

3. (a) F. Mansfeld, "Electrochemical Methods for Atmospheric Corrosion Studies," Proc. Symp. on Atmospheric Corrosion, the Electrochemical Society, Hollywood, Florida, October 1980 (in press); (b) F. Mansfeld, ASTM STP 727, 215 (1981).

4. F. Mansfeld. "New Approaches to Atmospheric Corrosion Research Using Electrochemical Techniques," in "Corrosion Processes," R.N. Parkins, ed., Appl. Sci. Publ. England, 1, (1982).

5. P.H. Sereda, ASTM, Bulletin No. 246, 47 (1960); P.J. Sereda, Ind. and Eng. Chem. 52(2), 157 (1965); P.J. Sereda, ASTM STP 558, 7 (1974).

6. V. Kucera and E. Mattson, ASTM STP 558, 239 (1974); V. Kucera and J. Gullman, ASTM STP 727, 238 (1981).

7. S. Haagenrud, Werkstoffe and Korrosion 31 (1980).

8. (a) Yu.N. Mikhailovskii, L.A. Shubakhina and C.T. Hong Wang, Proc. Metals 9, 135 (1973); (b) Yu.N. Mikhailovskii, G.B. Klark, L.A. Shuvakhina, V.V. Agafonov and N.I. Zhuraveleva, Prot. Metals 9, 240 (1973); (c) Yu.N. Mikhailovskii, P.V. Strekalov and V.V. Agafonov, Prot. Metals 16, 308 (1980).

9. F. Mansfeld and J.V. Kenkel, Corr. Sci. 16, 111 (1976).

10. F. Mansfeld and J.V. Kenkel, Corrosion 33, 13 (1977).

11. F. Mansfeld, Werkstoffe und Korrosion 30, 38 (1979).

12. F. Mansfeld and S. Tsai, Corr. Sci. 20, 853 (1980).

13. F. Mansfeld, "Evaluation of Electrochemical Techniques for Modelling and Monitoring of Atmospheric Corrosion Phenomena," Final Report to National Science Foundation, Grant No. DMR-7923965, May 1981.

14. F. Mansfeld, "Regional Air Pollution Study, Effects of Airborne Sulfur Pollutants on Materials," EPA-600/6-80-007, U.S. Environmental Protection Agency, Research Triangle Park, NC 27711, January 1980.

15. F. Mansfeld, "Results of Thirty Months Exposure Study in St. Louis, MO," CORROSION/78 Paper No. 88; Proc. 7th Int. Cong. Metallic Corrosion, Rio de Janeiro, Brazil, Paper No. 193, October 1978.

16. P.J. Sereda, S.G. Croll and H.F. Slade, ASTM STP 767, 267 (1982).

17. F. Mansfeld, "The Polarization Resistance Technique for Measuring Corrosion Currents," Adv. in Corr. Sci. and Tech. 6, 163 (1976), Plenum Press.

18. A.B. Harker, F.B. Mansfeld, D.R. Strauss and D.D. Landis, "Mechanism of SO_2 and H_2SO_4 Aerosol Zinc Corrosion," EPA-600/3-80-018, January 1980.

19. A.B. Harker, "Particulate Matter Soiling of Materials," Final Report SC5268.16FRD, November 1981.

APPENDIX I
PROCEDURE FOR PERFORMING ATMOSPHERIC CORROSION RATE MEASUREMENTS

1.0 SUMMARY

Corrosion rates are calculated from the electrochemical data collected from ACRMs which are exposed in a test chamber. These measurements are carried out as a function of relative humidity (RH), nature and concentration of various gaseous pollutants, carbonaceous material and aerosols.

2.0 EXPERIMENTAL PROCEDURE

2.1 Typical Test Sequence

The test sequence typically starts with installation of the sensors in the test chamber. The electrical connector to the corrosion current measuring amplifier, which is mounted on the sensor, is attached to the baseplate feed-through. The quartz jar of the test chamber, which is sealed with an O-ring to the baseplate, is installed. The polarization resistance for each sensor is measured with a computerized system, while the gas composition in the test chamber is selected by rotameter settings of the manifold. The gas composition is analyzed by the monitors and recorded by the computer. R_p for each sensor is monitored continuously while environmental parameters are varied. The data are stored on tape and analyzed after the test.

2.2 Measurement of Corrosion Rates

2.2.1 Collection of Electrochemical Data

The corrosion rate is determined from the current which flows when a potential difference of ±30 mV is applied to the sensors. The sensors are constructed as a two-electrode system with both electrodes made of zinc. The

substrate is a 0.25 mm (0.010 in.) thick epoxy laminate. The current which flows when the potential pulse is applied is a measure of the rate of the electrochemical corrosion reactions occurring at the metal/electrolyte/test atmosphere interface. The reaction rate is determined by the nature and concentration of the contaminants on the surface of the zinc and by the relative humidity, which provides the electrolyte and the conductivity between anodes and cathodes. The electrodes alternate as anode and cathode as +30 and -30 mV are applied.

The corrosion current I_{corr} is calculated from the applied emf ΔE of ±30 mV and the resultant current flow ΔI by:

$$I_{corr} = \frac{2B}{\Delta E} \Delta I = k \Delta I \quad ,$$

where B depends on the Tafel slopes (2). The integrated corrosion rate can be computed and converted to mass loss using Faraday's law. An electron charge of two is assumed from the anodic dissolution of zinc:

$$Zn \rightarrow Zn^{2+} + 2e \quad .$$

2.2.2 Measurement Principle

The current flow in response to a voltage pulse of ±30 mV is measured by a current measuring amplifier (Analog Devices AD517JH) which is an integral part of the sensor assembly. The voltage output of the amplifier, which is proportional to the current, is measured by an HP9825 desktop computer/HP6940 multiprogrammer system. The multiprogrammer D/A card is programmed to output ±30 mV simultaneously to as many as eight sensors. Sequential measurements of the currents on each sensor are made during each pulse using relay cards in the multiprogrammer with the output from the relay cards being measured by an

A/D. The current-time curves are stored on cassettes for later analysis. The polarity of the applied 30 mV emf is changed at the end of the 2 min pulse.

2.2.3 Sensor Preparation

The zinc sensors are cleaned by degreasing in ethanol. Pretreatment following cleaning consists of application of a known volume of deionized water, 1 mm NaCl or 1 mM $CaCl_2$ to which a small amount of alcohol has been added to improve wettability. One set of sensors had no pretreatment after cleaning. The liquids placed on the surface of the sensors are allowed to dry out and the sensors are kept overnight at 45% RH to age before use.

When carbonaceous particulate matter (CPM) is deposited on a sensor surface, it is applied in a separate step before the corrosion testing. Graphite, the CPM used in this test, is deposited using an Environmental Research Corporation Model 7330 fluid atomization aerosol generator. A dilution gas of dry air is added to the aerosol which consists of dilute ammonia in water to prevent forming of condensate on the sensor surface. Instead, dry graphite particles are deposited to reduce corrosion of the sensor during deposition of CPM.

The particulate loading used corresponds to a 6-month exposure to an urban environment (1). As measured with a reflectance meter, the reflectance change of white painted coupons exposed with the sensors is used to determine the particulate loading. The particle size distribution for the deposition of graphite under these conditions has been determined by Harker (1). The mass mean median diameter as measured by the electrostatic aerosol analyzer was 0.41 μm.

2.2.4 Weight Loss

Corrosion rates of zinc coupons prepared with the same cleaning and pretreatment procedure as the sensor were also determined by weight loss. One coupon accompanied each sensor for the duration of a test for comparison of weight loss data with electrochemical corrosion rate data. Because of locally

corroding anodes and cathodes on the surface of the zinc, uncompensated ohmic drop and other factors, not all of the corrosion is measured in the electrochemical test. The efficiency for copper/steel atmospheric corrosion monitors (ACMs) has been found to be about 20%, while for steel/steel ACMs, it was only 7% (3). Such correlations have not been made for zinc/zinc sensors. It was observed that for most tests which were of short duration (a few hours) the weight loss was too small to be measured accurately.

2.3 Operation of the Atmospheric Corrosion Gas Manifold

2.3.1 Setting of Flow Rates

The gas manifold provides the proper test atmosphere by mixing known volumes of gases. As shown in the manifold schematic (Fig. 1), the gases are metered by rotameters. Air dried by a desiccant and air humidified in two gas dispersion tubes are mixed and passed through an ozone generator (SOG-2 Ultraviolet Products, Inc.) and a gas mixing tube. The amount of ozone produced is a function of the exposed length of the ultraviolet lamp and the air flow rate. To this mixture analyzed mixtures of NO_2 and SO_2 can be added.

2.3.2 Setting of Gas Concentrations

The composition of gases in the test chamber varied from the inlet composition because of adsorption and/or reactions involving the various species. By measuring the concentration of SO_2, NO_2, ozone and relative humidity at the test chamber vent, suitable corrections to the nominal composition can be made to achieve the desired composition in the test chamber. The gas concentrations are measured by the monitors on the test chamber vent (see Fig. 1). Once the corrections to the nominal composition had been determined for the individual gases, these rotameter settings and ozone lamp settings were used to produce the desired gas compositions for single or multiple pollutants.

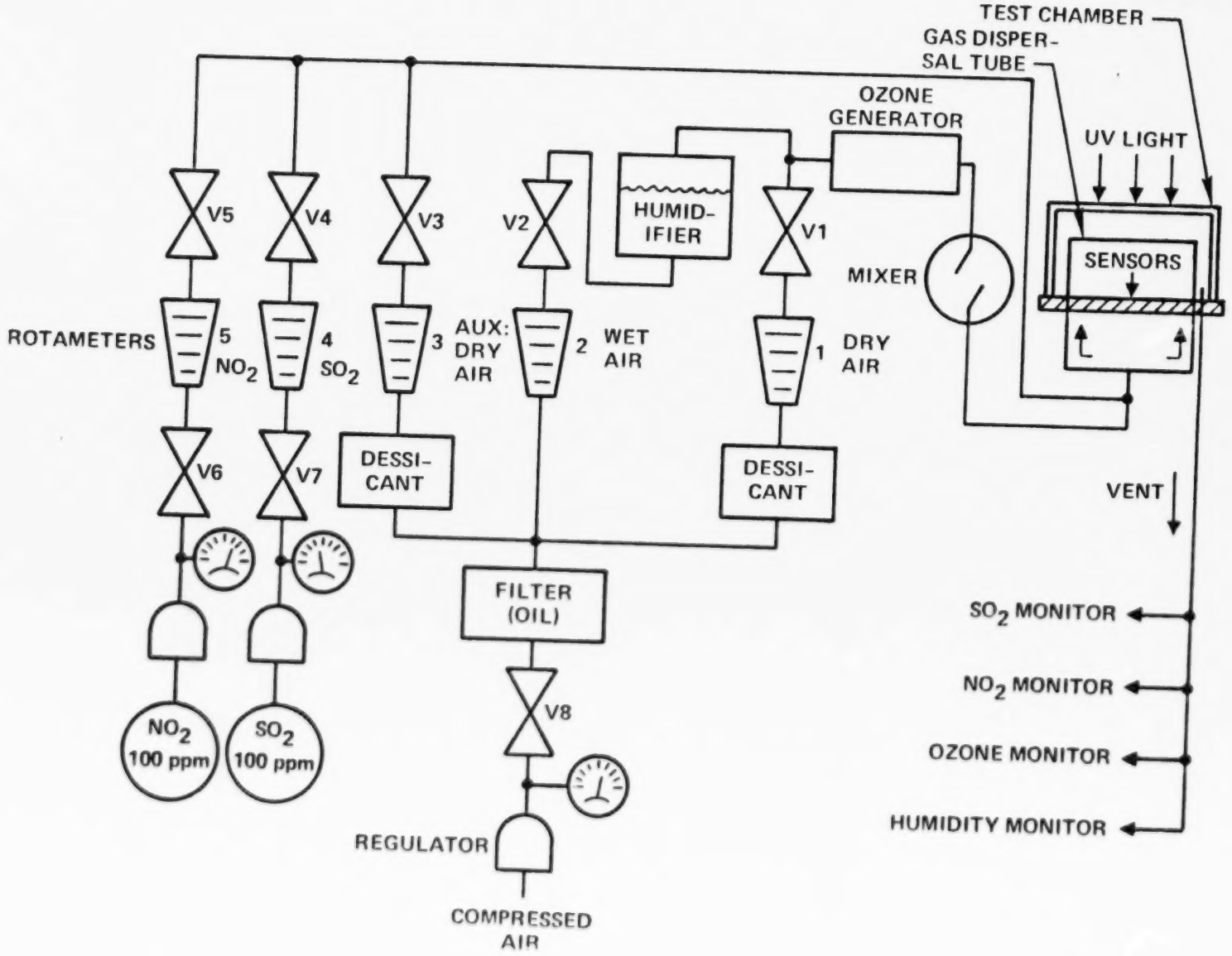

Fig. 1 Atmospheric corrosion gas manifold.

2.3.3 Calibration of the Rotameters

The rotameters were calibrated against a wet test flow meter for 1-4 l min^{-1} flow rates and against a bubble (soap film) flow meter for lower rates. A gas dispersion tube was used to saturate the gas with water before passing into the bubble flow meter. A regulated pressure of 16 psig air was applied to the rotameter inlet. The rotameter valves were installed on the outlets to minimize effects of pressure changes downstream of the rotameter due, for example, to the gas dispersion humidifier.

Flow rates of dry air at STP (V_s) were computed by:[4]

$$V_s = \frac{(P - p)}{Tt} \frac{273.2}{760} V, \text{ cm}^3 \text{ s}^{-1}$$

where P = total pressure of wet gas (barometric pressure) mm Hg
p = vapor pressure of water at T (°K), mm Hg
T = temperature of bubble meter or wet test flow meter, °K
t = time to sweep volume V of gas, s
V = bubble meter tube or wet test flow meter volume, cm^3

2.4 Operation of the Aerosol Generator

The corrosive effects of a weak acid (acetic) and a strong acid (sulfuric) in an aerosol having a mean particle size of about 1.9 μm were examined. The aerosol was produced by a collision nebulizer and passed into the test cell through Teflon tubing.

2.5 Operation of the Solar Lamp

Most of the expected light-induced reactions on a metal surface are produced by ultraviolet radiation. To supply a high UV flux, a 75 watt mercury lamp was used. A 45° mirror reflects the beam through the quartz jar and onto the surface of the sensors.

3.0 REFERENCES

1. A.B. Harker, "Particulate Matter Soiling of Materials," EPA Contract No. 68-02-3422, May 1982.

2. F. Mansfeld, in "Advances in Corrosion Science and Technology," Plenum Press, New York 6, 1563 (1976).

3. F. Mansfeld, et al, "Reproducibility of Electrochemical Measurements of Atmospheric Corrosion Phenomena," ASTM Special Publication 767, 309 (1982).

4. A. Levy, J. Sci, Instruments V41, 449 (1964).

APPENDIX II
ATMOSPHERIC CORROSION RATE METER AND DATA LOGGER (ACRMDL)

David K. Roe
Department of Chemistry
Portland State University
Portland, OR 97207

SUMMARY

A battery-powered meter and data logger has been designed and constructed for use with atmospheric corrosion sensors. This "meter" incorporates a small computer which is programmed in Basic language and which has sufficient memory to log 4,608 measurements from six sensors over a four-day period. A printer/plotter is used to provide hard copies of the results as log (impedance) vs time in tabular and graphical form. Results may also be transferred to cassette tape and to other computers via an RS-232C interface which is available from the computer manufacturer.

SPECIFICATIONS AND OPERATIONAL CHARACTERISTICS OF ATMOSPHERIC CORROSION RATE METER AND DATA LOGGER

The complete instrument, referred to as "ACRMDL," consists of four subunits:

1. Micro or pocket computer, Model PC-3 (Radio Shack) with 8K byte memory expansion.
2. Printer/plotter/cassette interface, Catalog No. 26-3605 (Radio Shack).
3. Digitally-controlled potentiostat, logarithmic current converter, analog-to-digital converter, Model PC-2 (Radio shack).
4. Rs-232C interface, catalogue No. 26-3612

Three battery chargers are included: Radio Shack 26-3605 operates the printer interface, 26-3612 operates the computer or the interface, and the

Gates 0813-4011 operates the circuit in subunit 3. Chargers have different size connectors and cannot be interchanged.

In the initial design stages of this instrument, a microprocessor board was planned. After a review of the many boards available and their suitability for the application, it became apparent that the new generation of "pocket" computers were vastly superior in ease of use and cost. The model selected has all of the necessary input/output connections conveniently available for data acquisition. Also it has a complete set of Basic instructions with many embellishments only found on larger computers. User memory is 10,042 bytes which is adequate for storage of the program (2,600 bytes), variables used in program execution and memory for sensor currents. Contents of memory are not lost when the computer is off as long as the batteries are operating (>1.2 v each). Battery life is ca. 100 hrs. of actual program operation but is measured in terms of shelf life when not processing a program. Batteries may be exchanged without loss of program or data by using the AC adapter.

Corrosion rate data is loaded from an 8 bit A/D converter directly into memory as a single byte. This technique allows a large number of measurements to be recorded in the available memory (768 measurements of each of six sensors, or 4,608 total). In addition new measurements are compared with the previously recorded values and if the change of all sensor currentsis less than ± 2 LSB (least significant bit) the new results are not stored, but instead a time memory byte is incremented by one bit. This storage technique greatly extends the usefulness of the available memory since in the present application it is expected that the sensors' output will change only slowly with time.

A complete listing of the program is given in Appendix A along with comments. Each section of the program is initiated by a function key (F1 to F6) so that no knowledge of programming or of this computer is required to properly use ACRMDL. There are six parts of the program and the purpose and function is described in the following.

F1. This key initiates the system by setting the sensor potential to zero and the parameters to the following values: pulse time = 120 s, pause between pulses = 120 s, delay time = 60 s, and pulse potentials to +30 mV and -30 mV. Display reads "READY" after the parameter are set. At this time sensor may be connected to the system. To start measurement cycles, press F3.

F2. If parameter values which are different from the defaults values above are desired, the operator is prompted by this routine. After each prompt, the numerical value is typed followed by pressing the ENTER key. When "READY" is displayed, the sensor may be connected and F3 pressed to start the measurements.

F3. Pressing this key initiates the measurement phase of the program which may extend from minute to days. During the first pulse, the value of the applied potential is displayed; default value is "+30 mV". At the end of this time, each sensor is sampled four times and the logarithium of the sensor current is averaged and placed in temporary storage. Each measurement requires about 2 ms. After all six sensors are serviced, the display shows the value of log Z of the six sensors in order. Because the display capacity is 26 characters and each result requires three digits and a space, the decimal points have been omitted. So if log Z = 4.32 for sensor no. 1, the display shows 432.

At the end of the first pause period, the applied potential is -E, as shown on the display. Sensor currents are recorded as before and displayed during the second pause period.

During the delay time, the results obtained during the +E and -E pulses are averaged, compared with the results already stored and a decision is made if the new results should be stored or not, based upon two criteria:

1. The available memory space is the first one in the three sections of the matrix (measurements number 1, 257 and 513).

2. The difference of any one sensor current is greater than ±2 in the least significant bit from the previously recorded values. If either of these two conditions is met, the results are stored. If not, then a seventh column of the memory matrix is incremented by one bit to indicated that the present cycle gave results that are the same as the previous results. Memory space is conserved by this technique and in the read out of the results, the true elapsed time is preserved. Display shows "No Impedance Change" during the delay time if there was no significant change and "Impedances Stored" if there was a significant diffe

Termination of the measurement cycle occurs when the memory is full. Elapsed time may be calculated from

$$ET = 768\ (4PT + DT)/3600 \text{ (hrs)}$$

where PT is pulse/pause time and DT is delay time. With the default values of PT and DT, 115.2 hours will be required to fill the memory, assuming there is a significant change each cycle.

Pressing the ON/Break key will halt or terminate the program. If done during the final step of the cycle, the last measurement will be valid.

F4. Tabular readout of the data requires the computer be connected to the Plotter/Cassette Interface (computer must be OFF during transfer, or memory may be scrambled), then ON key followed by F4 are pressed. An example of the copy is given below. Note that Start Time is given as MMDDHH.MMSS in order of month, day, hour, minute, seconds; leading and trailing zeros are not printed.

Considerable time and paper are required for a full print-out of the memory. The AC power adapter should be plugged into the printer during extended printing times.

F5. Graphs provide a concise readout of atmospheric corrosion rates and this program section makes use of the plotting capabilities of the Printer/ Cassette Interface. Again, note that the transfer of the computer must be made while OFF. Each graph displays log Z vs.time of three sensors in different colors and line styles, as shown below. The data are fitted to a time axis from the following possibilities: 1, 2, 5, 10, 20, 50, 100, 200, 500 and 1000 hours. Resolution of the plot is 0.2 mm on each axis.

Instructions for changing the paper roll and pens are in the Owners Manual, pp 12-20.

F6. This program loads the first 101 memory locations with synthetic data to demonstrate or check the plotting and print out programs.

Finally, it is evident that changes in the program are easily made using Basic. There are about 500 bytes available for expansion and changes. Type UNLOCK, press ENTER to enter program mode with MODE key.

A cassette recording of the complete program is included in case of accidental loss of program. If the computer becomes completely unresponsive after program loss, follow the procedure on p 21 of the PC-2 Owner's Manual, then type NEW Ø, press ENTER key. Connection of a cassette recorder (any reasonable quality one will suffice) is given on p. 22 of the Interface Manual, and loading instructions are on p. 33-34. The filename of the program is "ACMDA". Program is recorded from 3 to 75 on both sides of the cassette. After loading, rewind and repeat with the instruction CLOAD? "ACMDA" to varify proper transfer. If error message appears, repeat loading procedure, perhaps at higher volume setting.

Data may be transfered to cassette tape using the command PRINT # A(*) and the procedure on p 32. Again, the typing of RMT OFF and ON is not necessary when REM Ø jack is used. Recorded data may be reloaded with the command INPUT # A(*).

An RS-232C interface is available for the PC-2 which will allow serial transfer of data to another computer with the same interface capability. The Radio Shack Catalog No. is 26-3612 and from Sharp it is Model CE-158.

Circuit Description

Control and data acquision circuitry for the ACRMDL was designed with low power CMOS integrated circuits for extended battery life. It is housed in a 20 x 23 x 15 cm aluminum case which includes sufficient battery capacity (two Gates 0810-0017 sealed 6V, 2.5 AHR batteries in parallel) for about 4 days of continuous operation. A battery charger is included and the circuit may be operated with the charger connected; do not leave the charger connected beyond recommended times.

Up to six atmospheric corrosion rate sensors can be plugged into the circuit using readily available stereo phone plugs. Potential pulses are applied to the sensors according to the computer program and logarithms of currents are measured at the end of the pulse when currents are steady, as shown by previous laboratory studies. A potential-time waveform is diagrammed below for the default values.

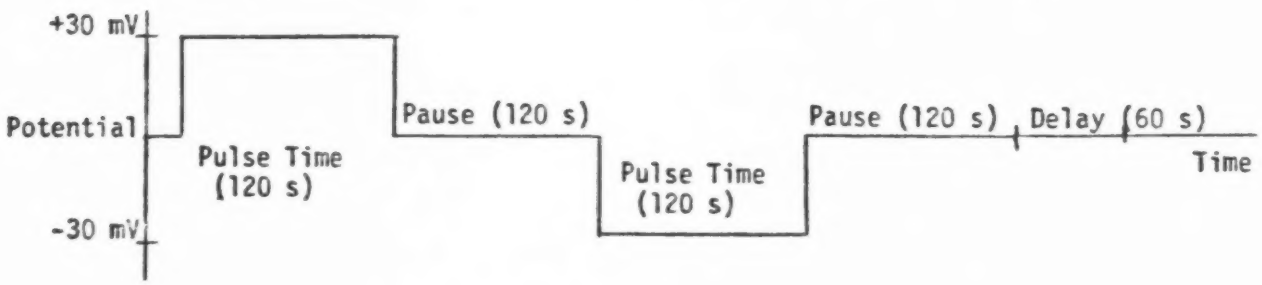

Other values of potential and time may be selected from the range of 0 to ± 127 mV and 1 to 1000 s. Pause time at the end of each pulse is equal to the pulse

time.

Potential pulses between + 127 and -127 mV are obtained from an 8-bit DAC in response to the computer program. The DAC sets the output of an op amp which is connected to one terminal of all six sensors; the other sensor terminals are grounded through six CMOS switches. At the end of the pulse time, the computer selects each sensor in order and one of its terminals is connected to a log current amplifier. The output of the amplifier is offset to agree with the input range of an 8-bit ADC and the value of log current is digitized four times in succession and placed in temporary storage in the computer. Conversion time for 24 measurements is about 50 ms.

There are two log amplifiers in the circuit so both positive and negative currents may be measured, but their outputs are adjusted to be in the same voltage range. Thus the circuit provides the logarithm of the absolute value of the sensor current. Range of the log amps is from 1 n A to 100 μA, giving 0 to 5 v, with a typical accuracy of 1%, rising to 5% at the low end. The equation relating the digitized log amp output (DLA, on a scale of 0 to 255) to sensor impedance, Z, is

$$\log Z = 6.005 + \log E - DLA\ (5/255)$$

Where E is in millivolts. Thus the range of log Z is from 2.48 to 7.48 if E = 30 mV. By using 6.005 instead of the expected 6.000, a rounding error is avoided. Resolution of log Z is limited by the quantizing error of the 8-bit ADC and it is ± 0.02, independent of sensor current because of the use of log amps at the input stage. Absolute accuracy is about twice the resolution over the full five-decade range, but the resistances of the analog switches become a limiting factor to accuracy; their resistance is about 300 Ω

Circuit diagram and component location are given in Appendix B.

Calibration Procedure

To check if calibration is needed, plug in the four dummy sensors in order of increasing resistances from 10 kΩ, to 10 MΩ . Connect the battery charger if batteries are not fully charged. Connect the computer (OFF connection) to the circuit (also OFF). Switch on the circuit, then the computer and press F2. Enter the following: dE = 127 mV, PULSE TIME = 10 s, DELAY TIME = 2 s, then press F3. If displayed values of log Z differ by more than ±0.05 from indicated values, on average, calibration is necessary.

Press OFF key of the computer, switch OFF circuit. Remove computer and the four screws holding the panel in place. Lift the panel clear of the case by raising the back edge and moving it toward the hinges. Place the case on its left side to allow enough lead length from batteries. Slide the computer in place, now the assemble will stand on the lower edge of the panel.

Locate the green DIP switches and switch OFF 1 and 2, then switch ON 7 and 8. Switch ON the circuit, not the computer, and connect the common lead of a DMM set for 10 V range to test point 7 and the input lead to TP1. Adjust P1 for an output of -3.2 to -3.5 V. Connect DMM input to TP2 and adjust P2 for an output between +3.2 and +3.5V. Leave circuit ON.

Reset the DIP switches (1-4 ON, 5-8 OFF) and press ON key of computer. Initiate test of dummy sensors as before. Connect DMM input to TP5 and note the values of applied potential during positive (+127 mV) and negative (-127 mV) cycles. Adjust P6 to change the pulse magnitude and adjust P5 to obtain symmetry.

While the computer is running, note the four values of log Z after the positive cycle and adjust P3 to bring them into specification of ±0.05, on average. Clockwise adjustments increase the readings. Typical measurements are: 4.04, 5.00 5.99, 6.95. Adjustment of the log Z values from the negative cycle are made with P4 and typical readings are as above. Remember that quantizing errors can occassionally cause a measurement to change by 1 bit which becomes a change in log Z of 0.02.

After completing the adjustments, press ON to BREAK the program, then press OFF key. Switch off circuit, separate computer from panel and refasten panel to the case.

Circuit Specification at 25°C

Potentiostat

Output voltage: -127 to +127 mV

Resolution: : 1 mV

Accuracy : ± 1 mV

Output current: ± 5 mA

Rise Time : about 5 ms

Log Amplifiers

Current Range: 1 nA to 100 µA

Accuracy : ± 1% to 10 nA, ± 5% at 1 nA

Output Voltage 0 to 5 V with bias provided by O A1-3.

Analog to Digital Converter

Input Range: 0 to 5 V

Resolution : 1 part ion 256 (8-bit)

Accuracy : ± 1 bit

Analog Switches, C MOS

Resistance ON: typically 200 to 300 ohms

Resistance OFF: Typically 10^{10} ohms

Impedance Measurement Accuracy

log Z from 4.00 to 7.00: ±0.05

Z from 1k to 10 M ohm: ± 10% + 200 ohms (due to analog switches)

log Z from 7.00 to 8.00 : ±0.05 to ±0.1

Power Requirements

50 mA at 6 V

Battery Supply Requirements

Two 6 V lantern batteries in parallel; Gates 0810-0017 sealed batteries supplied; capacity 2.5 AH each, or four-day continuous operation to cut-off voltage of 5.6 V. With charger connected, operation is unlimited.

Charging time

For each hour of use, charge with Gates 0813-4011 charger for one hour. Do not overcharge or leave charger connected when not in use.

"ACMDA"
Atmospheric Corrosion Meter and Data

Acquisition Program - D.K. Roe

```
 10:CLEAR :E=30:U=
    120:W=60:GOTO
    30
 20:CLEAR :INPUT "
    dE(mV)=?";E:
    INPUT "PULSE T
    IME(s)=?";U:
    INPUT "DELAY T
    IME(s)=?";W
 30:POKE# 32766,12
    8:PRINT "READY
    ":STOP
 40:U=1.5628E-2:
    DIM A$(20,255)
    *1:DIM B$(11)*
    1:S=TIME
 50:FOR Y=0TO 14
    STEP 7
 60:FOR Z=0TO 255
 70:C=0:POKE# 3276
    6,(128+E):WAIT
    INT ((U-.8)/U)
    :PRINT "dE=+";
    E;"mV":GOSUB 2
    00
 80:POKE# 32766,(1
    28-E):C=6:
    PRINT "dE=-";E
    ;"mV":GOSUB 20
    0
 90:FOR X=0TO 5:A=
    ASC B$(X):B=
    ASC B$(X+6):C=
    (A+B)/2:B$(X)=
    CHR$ INT C:
    NEXT X
100:WAIT ((W-.8)/U
    ):IF Z=0THEN 1
    50
110:FOR X=0TO 5:A=
    ASC A$((X+Y),(
    Z-1)):B=ASC B$
    (X):IF ABS (A-
    B)>2THEN 150
120:NEXT X
125:PRINT "NO IMPE
    DANCE CHANGE"
130:G=1+ASC A$((6+
    Y),(Z-1)):A$((
    6+Y),(Z-1))=
    CHR$ G:IF G=25
    5THEN 150
140:GOTO 70
```

Initiated by F1 Sets default conditions of E = 30 mV, pulse time = 120 s, delay time = 60 s.

Initiated by F2 Parameters can be entered over the following ranges: E = 1 to 127 mV; pulse time.= 1 to 1000 s; delay time = 1 to 1000 s.
Sensors may be connected at "Ready", E = 0 mV
Initiated by F3 Start time is recorded in S and storage matrix is dimensional

Positive E is applied to sensors for selected pulse time, then measurement subroutine is called.

Negative E is applied to sensors for selected pulse time, then measurement subroutine is called.

Log i values from positive and negative pulses are averaged.

Pause time between pulses started. Pause time is the same as pulse time.

Present measurements compared with previous set. If difference is > ±2 LSB, present set is stored in memory.

If difference is not > ±2 LSB, then "time" memory location is incremented one bit, "No Impedance change" is displayed during the pause between pulses, and a new measurement cycle is started. If "time" memory reaches 255, then measurement set is stored and a new memory address is indexed.

```
150:FOR X=0TO 5:A$
    ((X+Y),Z)=B$(X
    ):NEXT X
160:PRINT "IMPEDAN
    CES STORED":
    NEXT Z
170:NEXT Y
180:F=TIME :END
200:FOR X=0TO 5:
    POKE# (32760+X
    ),0:A=0
210:FOR D=0TO 3:
    POKE# 32759,0:
    A=A+PEEK# 3275
    9:NEXT D
220:A=A/4+.5:B$(X+
    C)=CHR$ INT A
230:NEXT X
240:POKE# 32766,12
    8:WAIT 1
250:FOR X=0TO 5:L=
    6.005+LOG E-(5
    /255)*(ASC B$(
    X+C)):PRINT
    INT (L*100);
260:IF X=4THEN
    WAIT ((V-.8)/U
    )
270:NEXT X
280:CLS :RETURN
```

Storage routine followed by "Impedances Stored". New measurement cycle is initiated.

Termination of measurement when memory full. Measurement routine at end of positive and negative pulses. Each sensor current is converted by ADC four times and averaged. Calculate values of log Z are displayed during the pause period between pulses. Decimal points are not included (5.32 displayed as 532). Range of possible values of log Z is from 2.5 to 7.5 for E = 30 mV.

Print out of Log Z versus Time

```
300:GOSUB 500
310:GRAPH :
    GLCURSOR (200,
    0):SORGN :
    ROTATE 1
320:LPRINT "TIME/h
    rs":GLCURSOR (
    -60,0):LPRINT
    "Log Z of":
    GLCURSOR (-90,
    0):LPRINT "Sen
    sor #"
330:FOR X=1TO 6:
    GLCURSOR (-30*
    X,-100):LPRINT
    X:NEXT X
340:GLCURSOR (0,-8
    0):SORGN :ET=0
    :MC=0
350:FOR MA=0TO Y
360:FOR ZP=0TO 255
370:ET=ET+(4*U+W)*
    (1+ASC A$((6+M
    A),ZP))/3600
380:GLCURSOR (0,-7
    0):SORGN :
    LPRINT .01*(
    INT (100*ET))
390:FOR X=0TO 5:
    GLCURSOR (-30*
    (X+1),0):L=6.0
    05+LOG E-(5/25
    5)*(ASC A$((X+
    MA),ZP))
400:LPRINT (INT (1
    00*L))*.01
410:NEXT X
420:MC=MC+1:IF MC>
    =(Z+256*Y)THEN
    450
430:NEXT ZP
440:NEXT MA
450:TEXT :LF 4:END
500:TEXT :LPRINT "
    START:";S
510:LPRINT "dE=";E
    ;"mV"
520:LPRINT "PULSE
    TIME=";U;"s"
530:LPRINT "DELAY
    TIME=";W;"s"
540:LF 2:RETURN
```

Initiated by F4 Start time and variables printed first according to subroutine 500.

Table format printed.

Elapsed time between changes in log Z calculated.

Values of log Z calculated from E and log i for each sensor.

Subroutine for printing start time and parameter values.

Plot of Log Z vs. Time

```
600:RC=0:MC=0:IF Y
    =21THEN LET Y=
    14
610:FOR MA=0TO Y
    STEP 7
620:FOR ZP=0TO 255
630:RC=RC+ASC A$((
    6+MA),ZP)
640:MC=MC+1:IF MC>
    =(Z+256*Y)THEN
    670
650:NEXT ZP
660:NEXT MA
670:TC=RC+MC:TT=TC
    *(4*U+W)/3600
680:IF TT<1THEN
    LET MD=.2
690:FOR SS=0TO 2:T
    S=TT*10^-SS
700:IF TS>1AND TS<
    2THEN LET MD=.
    4*10^SS
710:IF TS>2AND TS<
    5THEN LET MD=1
    0^SS
720:IF TS>5AND TS<
    10THEN LET MD=
    2*10^SS
730:NEXT SS
740:GOSUB 500
750:XD=0:GOSUB 800
760:GOSUB 500
770:XD=3:GOSUB 800
780:END
800:GRAPH :ROTATE
    1:GLCURSOR (10
    0,0):LPRINT "L
    og Z":GLCURSOR
    (-0,-80):SORGN
820:FOR DX=1TO 4
830:LINE (0,-100*D
    X)-(5,-100*DX)
    :GLCURSOR (5,-
    100*DX):LPRINT
    (DX*MD):NEXT D
    X
840:LINE (0,-400)-
    (0,0)-(200,0)
850:FOR DY=0TO 4
860:GLCURSOR (50*D
    Y,25):LPRINT (
    3+DY):LINE (50
    *DY,0)-(50*DY,
    -5):NEXT DY
870:FOR X=XDTO (XD
    +2):ZP=0:MA=0:
    RC=0
880:FOR CC=0TO (MC
    -1)
```

Initiated by F6 Lines 600 - 670 calculate the number of measurements stored and the number where there was no impedance change, then total time of measurement is calculated from pulse time and delay time.

Scale factor for time axis is determined from total time and the menu programmed: 1, 2, 5, 10, 20, 50, 100, 200, 500, and 1000 hours.

Parameter values printed
Plot of sensors 1-3 called
Parameter values printed
Plot of sensors 4-6 called
Plot subroutine. Lines 800-860 draw and label axes

Start of log Z vs. time plot

```
890:PC=X+1:PS=X:IF
    X)=3THEN LET P
    C=(X-2),PS=(X-
    3)
900:L=50*(3.005+
    LOG E-(5/255)*
    (ASC A$((X+MA)
    ,ZP)))
910:IF CC=0THEN
    GLCURSOR (L,0)
920:ET=(CC+RC+1)*(
    4*U+W)/(36*MD)
    :RC=RC+ASC A$(
    (6+MA),ZP)
930:MT=(CC+RC+1)*(
    4*U+W)/(36*MD)
940:LINE -(L,-ET)-
    (L,-MT),PS,PC
950:ZP=ZP+1:IF ZP=
    256THEN LET MA
    =MA+2,ZP=0
960:NEXT CC
970:NEXT X
980:GLCURSOR (5,-4
    50):COLOR 0:
    LPRINT "TIME/H
    rs":LINE (0,-4
    00)-(0,-500)-(
    5,-500)
990:FOR X=XDTO (XD
    +2):PC=X+1:PS=
    X:IF X)=3THEN
    LET PC=(X-2),P
    S=X-3
 1000:LINE ((156-2
      0*X),-560)-(
      (156-20*X),-
      600),PS,PC
 1010:GLCURSOR ((1
      50-20*X),-52
      0):LPRINT "#
      ";(X+1)
 1020:NEXT X
 1030:TEXT :LF 6:
      COLOR 0:
      RETURN
```

Log Z calculated from log A and E

End of plot routine
Sensor number and pen color identified

End of subroutine

Test Program
Initiated by F6

```
1100:CLEAR :DIM A
     $(20,255)*1:
     S=TIME
1110:FOR X=0TO 5
1120:FOR Z=0TO 10
     0
1130:A$(X,Z)=CHR$
     (2*Z+10*X)
1140:NEXT Z
1150:NEXT X
1160:A$(6,50)=
     CHR$ 10
1170:U=64:W=64:E=
     100:GOTO 600
```

101 memory locations are loaded to test or demonstrate the plot program

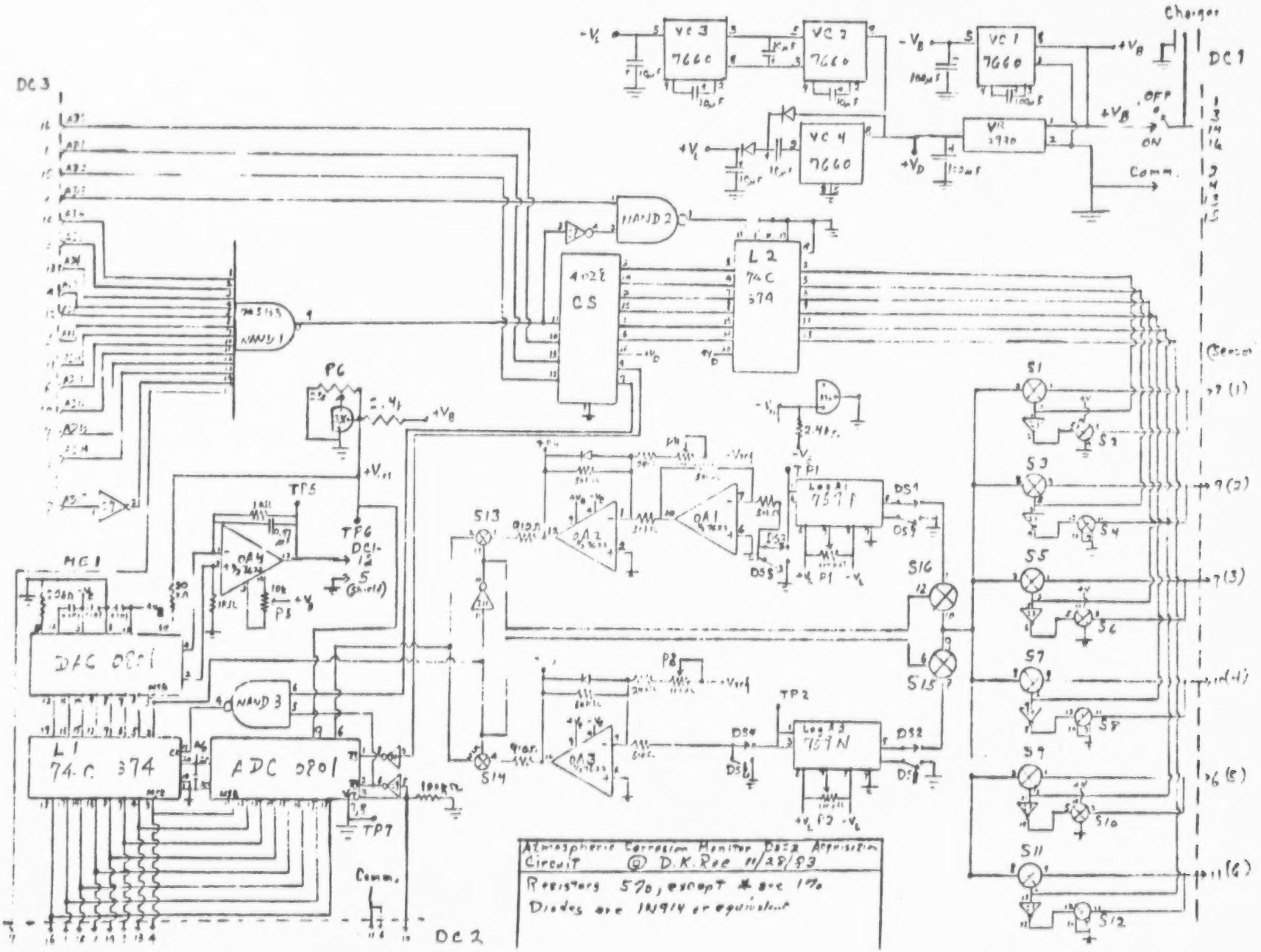
DC 3
DC 1
DC 2
Charger
VC 3 7660
VC 2 7660
VC 1 7660
VC 4 7660
VR 7930
HAND 2
NAND 1
NAND 3
4028 CS
L 2 74C 374
L 1 74C 374
DAC 0801
ADC 0801
MC 1
TP5
TP6
TP7
TP1
TP2
TP3
TP4
Log A1 7571
Log A2 7571
OA 1
OA 2
OA 3
OA 4
S1
S2
S3
S4
S5
S6
S7
S8
S9
S10
S11
S12
S13
S14
S15
S16
DS1
DS2
DS3
DS4
DS5
Comm.
OFF
ON
Atmospheric Corrosion Monitor DAS Acquisition Circuit © D.K. Roe 11/28/93
Resistors 5%, except * are 1%
Diodes are 1N914 or equivalent

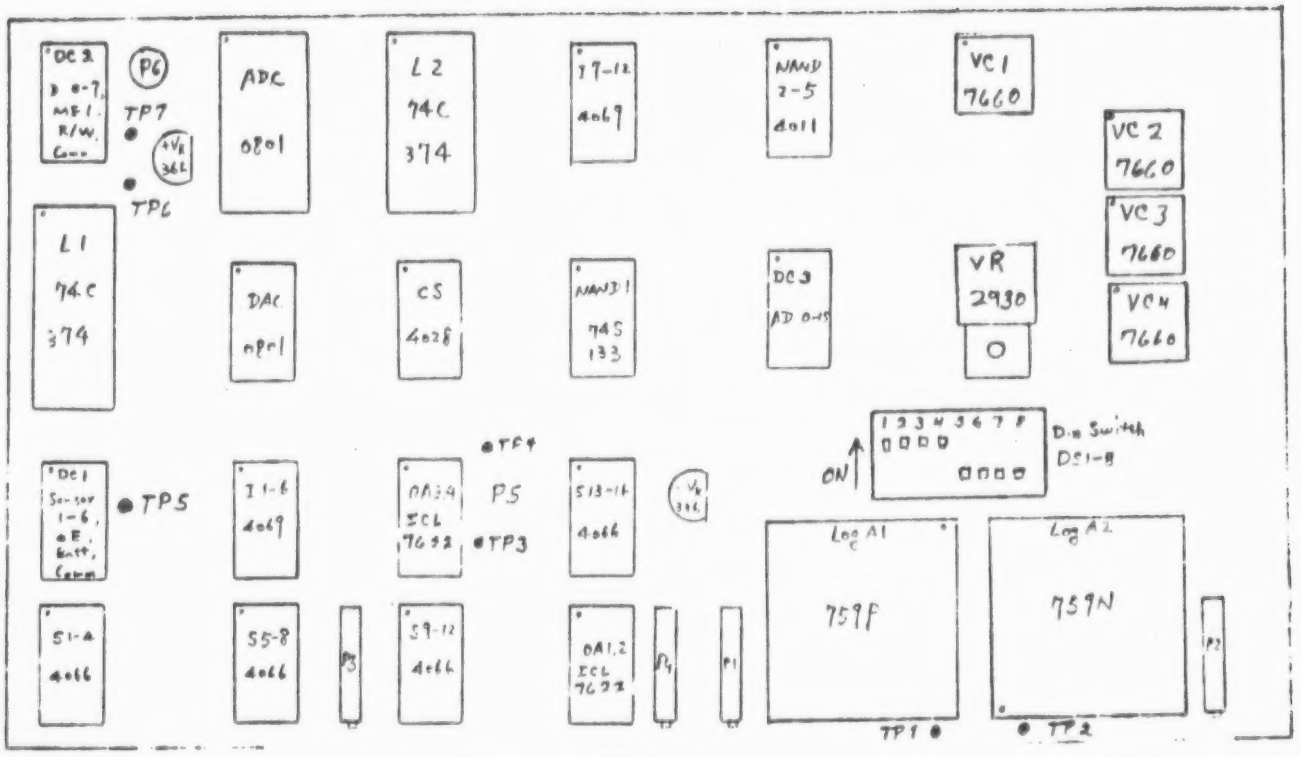

TOP VIEW

Atmospheric Corrosion Monitor Data Acquisition
Circuit - Component Location © D.K. Ree 11/20/83

Filter Caps not shown
Resistors not shown
* Indicates pin #1